

PAPER NAME

**Thesis-vishwajeet21mce217.pdf**

AUTHOR

**Viswajeet**

WORD COUNT

**8240 Words**

CHARACTER COUNT

**44304 Characters**

PAGE COUNT

**54 Pages**

FILE SIZE

**2.9MB**

SUBMISSION DATE

**May 22, 2023 10:57 AM GMT+5:30**

REPORT DATE

**May 22, 2023 10:58 AM GMT+5:30**

### ● 17% Overall Similarity

The combined total of all matches, including overlapping sources, for each database.

- 8% Internet database
- 6% Publications database
- Crossref database
- Crossref Posted Content database
- 16% Submitted Works database

### ● Excluded from Similarity Report

- Bibliographic material
- Quoted material
- Cited material
- Small Matches (Less than 8 words)

# **FINITE ELEMENT ANALYSIS AND OPTIMIZATION OF FLEXIBLE PAVEMENT LAYER THICKNESS**

<sup>18</sup>**M.Tech Thesis**

by

**Vishwajeet Kumar**

**(REGISTRATION NUMBER.21MCE217)**



**DEPARTMENT OF CIVIL ENGINEERING  
NATIONAL INSTITUTE OF TECHNOLOGY  
HAMIRPUR – 177005, INDIA**

**MAY, 2023**

# FINITE ELEMENT ANALYSIS AND OPTIMIZATION OF FLEXIBLE PAVEMENT LAYER THICKNESS

4 Thesis submitted in partial fulfillment of  
requirements for the Degree of

**Master of Technology**

by

**Vishwajeet Kumar**

**(Registration Number.21MCE217)**

*Under the guidance of*

**Dr. Sunil Sharma**



to the

**DEPARTMENT OF CIVIL ENGINEERING  
NATIONAL INSTITUTE OF TECHNOLOGY  
HAMIRPUR – 177005, INDIA**

**MAY, 2023**

**Copyright © NIT Hamirpur, HP, India,  
2023**



**NATIONAL INSTITUTE OF TECHNOLOGY**

**HAMIRPUR, H.P.**

**CANDIDATE'S DECLARATION**

I hereby confirm that the work<sup>41</sup> which is being introduced in the thesis entitled **“Finite Element Analysis and optimization of Flexible pavement layer Thickness”**

<sup>3</sup> in partial fulfilment of the prerequisite for the award of Degree of Master of Technology and submitted in the Department of Civil Engineering, National Institute of Technology, Hamirpur (H.P.), is purely my own record of the work done during the period from July, 2022 to May, 2023 under the supervision of **Dr. Sunil Sharma**, Assistant Professor Department of Civil Engineering, National Institute of Technology Hamirpur. To the best of my knowledge the matter introduced in this thesis has not been submitted to any other<sup>5</sup> degree of this or any other institute/University.

VISHWAJEET KUMAR

This is to certify that above statement made by candidate is correct to the best of my knowledge.

Dr. Sunil Sharma

Assistant professor

Civil Engineering Department

Date:

The M-Tech Viva-Voce Examination of Vishwajeet Kumar has been held on \_ \_ \_ \_

Signature of Supervisor

Signature of Internal  
Examiner

<sup>26</sup>Signature of External  
Examiner

## ACKNOWLEDGEMENT

I want to thank and recognise my supervisor, Dr. Sunil Sharma (Assistant Professor, Department of Civil Engineering, NIT Hamirpur, HP), who permitted me to accomplish this project. He provided guidance and advice that helped me at each step of writing my research paper. I like to express my sincere thanks to Professor Raman Parti for his valuable suggestions and critiques throughout the project.

I also like to give special thanks to my friends Waquar ahmad Siddiqui, murslim hoque, Rahul kumar, Amit kumar, Shivam kumar and my entire family for their unwavering support during the research process.

I also thank Mr. Nitin Paliwal and the rest of the employees of the library for their kindness, smiles, and support.

Finally, I intend to say my sincere thanks to God for steering me through all of my hurdles. Each day, I felt your guides. I'm able to complete my degree because of you. For my future, I'm going to continue placing my trust in you.

**Vishwajeet Kumar**  
**(21MCE217)**

# ABSTRACT

The flexible pavement is one of the vital modes of transport which are designed to be flexible and withstand heavy traffic loads.<sup>10</sup> The objective of current research is to investigate the structural characteristics of flexible pavement using techniques of Finite Element Analysis (FEA).<sup>42</sup> The FEA of flexible pavement is conducted using ANSYS simulation package.<sup>7</sup> From the structural FEA analysis on flexible pavement, the critical regions of high stresses and deformation are identified.<sup>1</sup> The contour plots on stresses have shown that the stresses are maximum at the contact region and at the zone of load application. The stresses and deformation are maximum at the wearing course and bituminous course.

**Keywords:** pavement design, finite element analysis, optimization, Response surface method, finite element method

# 15 CONTENTS

<b>CANDIDATE'S DECLARATION</b>	20
<b>ACKNOWLEDGEMENT</b>	ii
<b>ABSTRACT</b>	iii
<b>CONTENTS</b>	iv-v
<b>LIST OF FIGURES</b>	vi-vii
<b>LIST OF TABLES</b>	viii
<b>LIST OF ABBREVIATIONS</b>	ix
<b>CHAPTER 1</b>	1-10
<b>Introduction</b>	1
1.1 General	1
1.2 Structural components of a flexible pavement	2
1.2.1 Subgrade	3
1.2.2 Subbase Course	3
1.2.3 Base Course	3
1.2.4 Surface Course	3
1.3 Flexible Pavement Distress	3
1.3.1 Fatigue cracking	4
1.3.2 Block Cracking and Transverse (Thermal)	4
1.3.3 Potholes	5
1.3.4 Rutting	6
1.3.5 Longitudinal cracking	6
1.4 Stress distribution	7
1.5 Finite element method	8
1.6 FEM application	9
1.7 Finite element analysis software ANSYS	9
<b>CHAPTER 2</b>	11-16
<b>LITERATURE REVIEW</b>	11
<b>CHAPTER 3</b>	17
<b>Research gap and objectives</b>	17



3.1 Research gap	17
1 3.2 Objectives	17
<b>CHAPTER 4</b>	18-23
<b>Methodology</b>	18
4.1 Methodology	18
1 4.2 Methodology steps	19
4.2.1 CAD modelling	19
4.2.2 Meshing CAD modelling in ANSYS	21
4.2.3 Applying loads and boundary conditions	21
1 4.2.4 Solution stage	22
4.2.5 Response surface methodology for design optimization	22
<b>CHAPTER 5</b>	24-36
<b>Results and Discussion</b>	24
5.1 FEA results on pavement	24
1 5.2 Response surface optimization	27
<b>CHAPTER 6</b>	37
<b>CONCLUSION AND FUTURE SCOPE</b>	37
6.1 Conclusion	37
6.2 Future Scope	38
References	39-42

## 17 List of Figures

Figure No.	Figure Caption	Page No.
1.1	Schematic of a flexible pavement	2
1.2	Fatigue(alligator) cracking in flexible pavement	4
1.3	Block cracking (medium severity)	5
1.4	High severity pothole	5
1.5	Rutting	6
1.6	Longitudinal Cracking (medium severity)	7
1.7	Wheel load pressure distribution within the pavement structure	8
4.1	CAD model of pavement	19
4.2	CAD model of pavement	19
4.3	CAD model of pavement base layer	20
4.4	CAD model of pavement subgrade	20
4.5	Hexahedral element meshed	21
4.6	Loads and boundary condition	22
4.7	Variables definition for optimization	23
5.1	Maximin normal stress along X direction (horizontal direction)	24
5.2	Maximum normal stress along Y direction (vertical direction)	25
5.3	Maximum normal stress intensity	25
5.4	Total deformation plot	26
5.5	Total deformations plot across length	26
5.6	Normal stress along the length	27
5.7	DOE table generated	27
5.8	Shear stress vs design point	28
5.9	Normal stress vs design point	28
5.10	Total deformation vs design points	29

5.11	Goodness of fit curve	29
5.12	Shear stress vs subgrade	30
5.13	Shear stress vs baselayer	30
5.14	Shear stress vs bl	31
1 5.15	Normal stress vs subgrade	31
5.16	Normal stress vs baselayer	32
5.17	Normal stress vs bl	32
5.18	1 Total deformation vs subgrade	33
5.19	Total deformation vs baselayer	33
5.20	Total deformation vs bl	34
22 5.21	Response surface plot of shear stress	34
5.22	Response surface plot of normal stress	35
5.23	Response surface of total deformation	35
5.24	Sensitivity percentage block	36

# List of Tables

Table No.	Table Caption	Page No.
4.1	Optimization variables	23

## 21 List of Abbreviations

FEA	Finite Element Analysis
FEM	Finite Element Method
SA	Simulated Annealing
DOE	Design of Experiment
CBR	California Bearing Ratio
PCC	Portland Cement Concrete
RSM	Response Surface Method
IRC	Indian Road Congress
BL	Bituminous Layer
CFD	Cumulative Fatigue Damage
DBM	Dense Bituminous Macadam
BM	Bituminous Macadam
RAP	Reclaimed Asphalt Pavement
AV	automated vehicle

# CHAPTER 1

## INTRODUCTION

### 1.1 General

For a road to be built properly, it must have pavement. Its main purposes are to maintain a constant traffic flow, evenly distribute the weight, and ensure both vehicular and pedestrian safety. Even in asphalt parking lots, pavement performs a variety of crucial tasks that the general public occasionally takes for granted. The pavement can age over time and become less durable due to elements like the weather, heavy traffic, frequent use, and vehicle weight. This is especially true if regular maintenance does not extend the pavement's lifespan. It is well known that flexible pavement analysis is challenging due to the multi-layered, three-dimensional nature of the pavement system. The system must take into account the various properties of each layer in order to give accurate displacements, strains, and stresses.

A road needs pavement in order to be constructed properly. Its main goals are to maintain a steady flow of traffic, distribute the weight uniformly, and guarantee the safety of both vehicles and pedestrians. Pavement serves a range of essential duties that the general public occasionally takes for granted; even in asphalt parking lots. This is particularly true if routine upkeep does not lengthen the pavement's lifespan. It is well known that the multi-layered, three-dimensional character of the pavement system makes flexible pavement analysis difficult. For the system to provide accurate displacements, strains, and stresses, it must take into consideration the various attributes of each layer.

There are two basic kinds of road pavements; Rigid & Flexible. Commonly used as wearing surfaces on stiff pavements, Portland cement concrete acts as a beam over any flaws in the underlaying material. However, the bituminous materials used in flexible pavements ensure that even tiny abnormalities are kept in touch with the underlying subgrade. A bituminous base is covered with a granular and a fine layer of material to create flexible pavements. Instead of using a foundation course, concrete pavements are constructed using Portland cement concrete.

A road needs pavement in order to be constructed properly. Its main goals are to maintain a steady flow of traffic, distribute the weight uniformly, and guarantee the safety of both vehicles and pedestrians. Pavement serves a range of essential duties that the general public occasionally takes for granted, even in asphalt parking lots. This is particularly true if routine upkeep does not lengthen the pavement's lifespan. It is well known that the multi-layered, three-dimensional character of the pavement system makes flexible pavement analysis difficult. For the system to provide accurate displacements, strains, and stresses, it must take into consideration the various attributes of each layer.

## 1.2<sup>28</sup> Structural components of a flexible pavement

There are four components to flexible pavements: the subsoil, the subbase, the base and the surface course. The latter gets stiffer & contributes more to the pavement's strength when formed with Hot Mix Asphalt.



Figure 1.1: Schematic of a Flexible Pavement.

The pavement's performance is directly related to the quality of each component's performance.

## 1.2.1 Subgrade

It is the organic material that runs perpendicularly over the surface of pavement and serves as the structural support of pavement. In certain cases, the subgrade material must be treated to provide the needed strength attributes for the kind of pavement that is being created.

## 1.2.2 Sub-base course

An elevated layer of building material called a sub-base sit directly above the lower one known as a subgrade. Because of the quality of the subgrade material, it's possible to dispense with the sub-base material. Stabilization is a method of treating soils to enhance their technical features when the sub-base material does not meet the specifications. To get the desired qualities, the material must be combined with other material.

## 38 1.2.3 Base course

sub-base is placed on top of base course (or, if sub-base course is not used, above the subgrade). The majority of this material is made up of granular components, including sand, crushed or uncrushed gravel, and crushed or uncrushed slag. In general, prerequisite requirements for basic courses are more stringent than those for other courses. To increase stiffness, heavy-duty pavements may benefit from having the base course treated with asphalt or Portland cement.

## 1.2.4 Surface course

top layer of the pavement segment, directly above base course, is known as the surface course. Mineral aggregates asphaltic materials are generally used in surface course of flexible pavements. There are several things that might cause the pavement to degrade faster; therefore it has to be resistant to them all.

## 1.3 Flexible Pavement Distress

Cracking, rutting, potholes, and surface degradation are among the most typical problems with flexible pavement. According to the definitions from the LTPP Distress Identification Manual and the US Department of Transportation's distress identification guidebook (Federal Highway Administration, 2003), a number of pavement distress classes are briefly addressed in this section.



### 1.3.1 Fatigue Cracking

In asphalt pavements with granular and poorly stabilized foundations, fatigue (also known as alligator) cracking is the most common structural problem. There are two types of alligator-cracking: parallel longitudinal fractures in the wheel tracks, and interconnecting cracks that resemble chicken wire. Localized failures and potholes may develop as a result of alligator cracking, especially in regions where the support is weak.

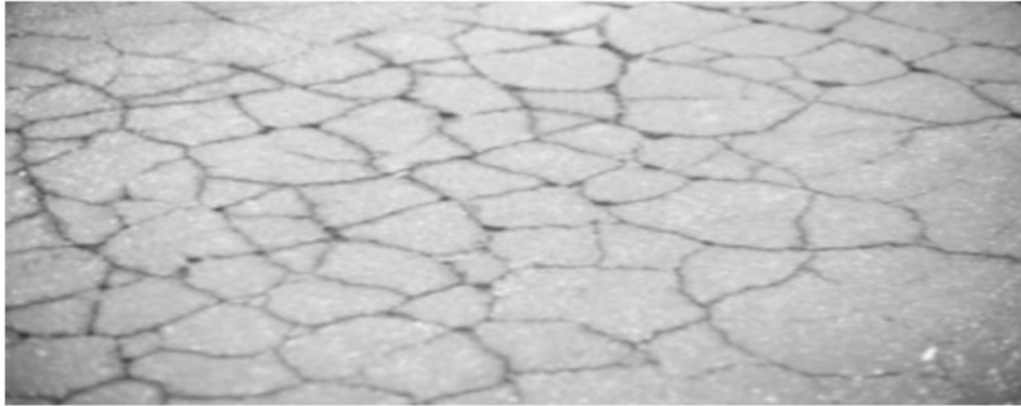


Fig 1.2: Fatigue (alligator) cracking in Flexible Pavement

The following are some factors that affect how alligator cracking develops:

- Application of loads, both in quantity and magnitude.
- The pavement's structural design
- Quality and consistency of the foundation;
- Asphalt is a kind of material.

### 1.3.2 Block Cracking and Transverse (Thermal)

Block cracking is the process of fracturing asphalt pavement into rectangular pieces that measure 30 to 300 cm on a side. Cracking develops in large paved surfaces like parking lots and highways, mainly in places that are not exposed to heavy traffic loads, although it may also occur in areas that are heavily used. In most cases, thermal fractures appear across the driving lanes of a highway.



Figure 1.3: Block Cracking (Medium Severity)

The use of asphalt that is excessively stiff for the environment leads to both block cracking and heat cracking. There are two different forms of cracking that occur when asphalt shrinks as a result of low temperatures. Using asphalt with a low stiffness is the best way to prevent block and thermal cracking (high penetration) .

### **1.3.3 Potholes**

An asphalt pavement pothole is a bowl-shaped hole between 15 and 90 centimeters in dia that occurs in one or more layers of the asphalt pavement construction. In alligator-cracked regions, traffic wheels move asphalt pieces, causing potholes to develop. With time, potholes expand in both size and depth, weakening the area around them as water gathers in the hole.



Figure 1.4: High Severity Pothole

### **1.3.4 Rutting**

Wheel path rutting occurs when material in the base or subgrade or asphalt layer moves or consolidates, causing a longitudinal depression in the road. There are a number of elements that might lead to deformation in subsurface layers, including asphalt thickness, stability of subbase layers, subgrade support quality, and the amount and kind of applied loads.



Figure 1.5: Rutting

### **1.3.5 Longitudinal Cracking**

Non-motorized route Longitudinal cracking in an asphalt pavement may be caused by insufficient compaction at the margins of longitudinal paving lanes, aged pavement edges, or edges and cracks in a stabilised foundation. The application of strong loads or high tyre pressures may also cause longitudinal cracking in the wheel tracks.

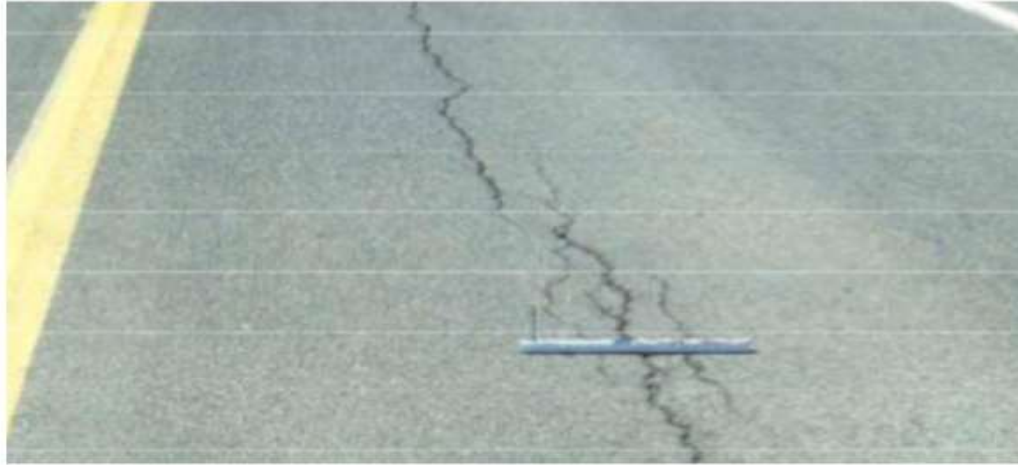


Figure 1.6: Longitudinal Cracking (Medium Severity)

## 1.4 Stress Distribution

A road structure's stress distribution is investigated to learn how phenomena emerge in the road structure and, in particular, to understand the behaviour of the asphalt layers. Stress distribution. An example of a wheel load pressing down on a road surface may be seen in Figure 1.7. Multiple layers of pavement minimise the weight by spreading it out and distributing it more evenly. The subgrade pressure,  $P_1$ , is much lower than the tyre pressure,  $P_0$ , on the surface of pavement. Higher grade materials are utilised in the top layers of all pavement systems, whereas lesser quality and less costly materials are used in the deeper levels of the pavement. Consequently However, if this criterion is not satisfied or if these layers are deteriorated, the pavement's resilience is severely diminished. Fissures, longitudinal cracks, alligator cracks, surface depreciation, and potholes are all possible outcomes of this.

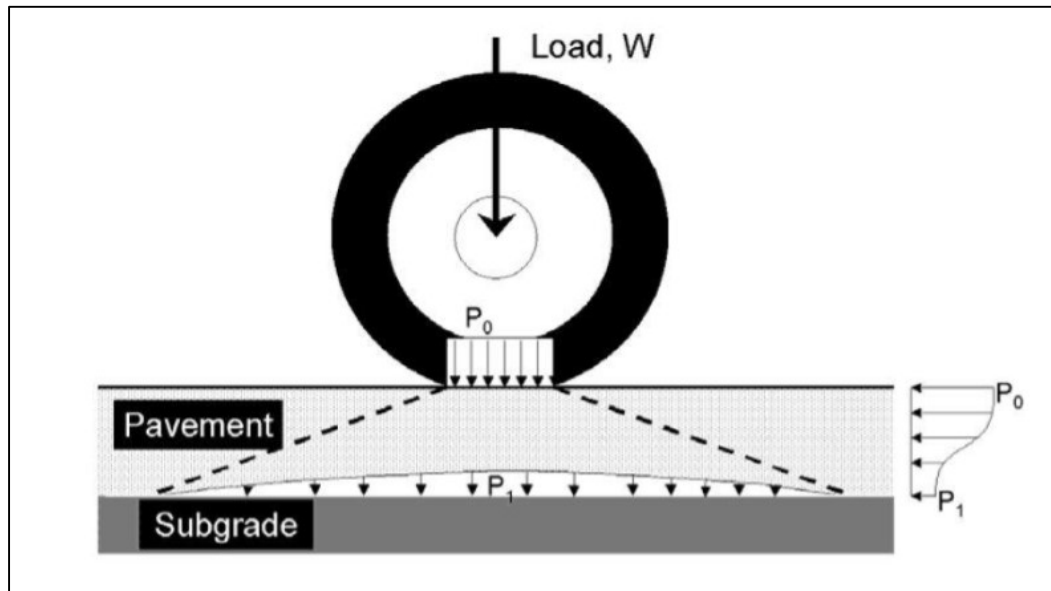


Figure 1.7: Wheel load pressure distribution within the pavement structure

During the accelerating and breaking phases, shear stresses arise on the pavement surface owing to tyre adhesion to the wear course, whereas the vertical forces are a result of the weight on the wheel. There is a lot of compression in the lower layers and plenty of bending in the top levels. More and more research has shown that stress distribution is really quite complicated since tensile development affects not only surface layers but also layers immediately underneath them, as has been shown in recent years by several studies.

## 1.5 Finite Element Method

- **Modeling.** The complex irregular shapes and geometries can be easily developed and analyzed. The critical regions of high stresses and other geometric factors affecting the results can be evaluated.
- **Adaptability.** The design cycle and cost of production can be reduced significantly as it reduces number of iterations. The hard prototyping stage can be removed.

- **Accuracy.** By increasing the number of iterations and using convergence techniques, the accuracy of solution can be improved.
- **Time-dependent simulation.** The transient structural analysis, transient thermal analysis can be conducted on different structures.
- **Boundaries.** The user can change boundary conditions easily as compared to experimental techniques. The thermal, structural and fluid flow conditions are easily changeable.
- **Visualization.** The FEA simulation package enables user to identify regions critical regions of high stresses, deformation and safety factor.

## 1.6 FEM Application

**1. Mechanical engineering:** In automobiles component design, machine component design and other tool design.

**2. Geotechnical engineering:** The geotechnical engineering involves soil stability, soil structure and fluid solid interaction. The analysis involves heavy structures like tunnels, dams etc.

**3. Aerospace engineering:** The aerospace engineering involves use of FEA in aircraft design, shuttle design. The type of analysis involves vibration and structural type.

**4. Nuclear engineering:** The safety and performance of nuclear reactor is investigated. The analysis of reactor involves steady state and transient state.

## 1.7 FINITE ELEMENT ANALYSIS SOFTWARE – ANSYS

Dr. John Swanson created the ANSYS software in 1970; it was originally known as ANSYS Inc. The founder of modern FEA is acknowledged as John Swanson, who created the simulation software. By extending its range of operations to encompass magnetostatics, kinetodynamics, piezoelectrics, electronics, CFD, structural, vibration, fatigue, and other optimisation approaches. A numerical method called the finite element method can be used to produce approximations of solutions to a range of engineering problems. The finite element method can be used to analyse difficulties in the development of models, stress analysis, steady-state, transient, linear, or nonlinear

problems in stress analysis. The finite element approach is not the only one that may describe a given domain as a set of discrete components. The perimeter of a polygon enclosed by a circle is said to be close to the circumference of the latter, which is how ancient mathematicians calculated the value approximations of solutions to vibration systems. A numerical method called the fem can be used to produce approximations of solutions to a range of engineering problems. The finite element method can be used to analyse difficulties in the development of models, stress analysis, steady-state. The finite element approach is not the only one that may describe a given domain as a set of discrete components. The perimeter of a polygon enclosed by a circle is said to be close to the circumference of the latter, which is how ancient mathematicians calculated its value. By imagining the circle as a polygon with an infinitely large number of sides, they were able to predict the value with an accuracy of almost 40 significant digits. The method is now much faster and simpler to use thanks to FEA systems' improved user interfaces, automated functionality, and excellent graphical capabilities. Despite these advancements, full-blown advanced FEA still takes a lot of effort and the skill of a committed analyst who is familiar with how to apply the right mesh densities, element kinds, and boundary conditions. These skilled analysts also need to be able to properly translate CAD geometry into the appropriate format for creating the FEA model and evaluate plots and other output data.

## CHAPTER 2

### LITERATURE REVIEW

**Khan (1998) [1]** The Group Index Method and the CBR Method are explored in relation to flexible pavement design. A soil's Group Index is used to estimate its thickness initially. Subgrade Group Index and thickness are presented in connection to different traffic conditions. Building depth and % of California Bearing Ratio Percentage are used in the construction of California Bearing Ratio curves.

**Arora (2003) [2]** Flexible pavement design strategies have been documented in a variety of ways. Methods such as McLeod's approach. Thickness of foundation and surface are linked to traffic volume in Group Index Method constructions. Light, medium, and heavy traffic are plotted on CBR and pavement thickness curves in the CBR Method. The CR Value Method employs the R-value, which stands for California Resistance. The McLeod Method utilises graphs to show the relationship between construction depth and CBR under various traffic scenarios.

**Punmia et al (2005) [3]** In this study, they report on the results of Burmister & elastic deformation analyses for flexible pavements. There have been produced charts for vertical deflections. Curves for the GI Method and the CBR Method have been made available for usage. This method uses the GI and the thickness of the line to plot the curves of the data. Using the California Bearing Ratio Method, a line is drawn from California Bearing Ratio to the thickness of a building's structure.

**Subagio et.al (2005) [4]** analyses the structural behaviour of many layers of pavement using approaches with an equivalent layer thickness. Multilayer pavement systems may be modelled using a one-layer pavement system having identical thicknesses of one



elastic modulus. The approach of equivalent thickness<sup>8</sup> is based on the premise that the stiffness of a layer affects the stresses and strains that occur underneath it.

**Das (2008) [5]** Mechanistics empirical approaches to bituminous pavement design are discussed in this paper. The reliability of a certain pavement may be evaluated using a variety of failure criteria that take into consideration variations in pavement design input parameters. Based on empirical pavement design methods, a technique has been proposed to design asphalt pavements with a certain degree of overall dependability.

**Tarefder et. al (2010) [6]** The diversity of design inputs necessitates consideration of dependability in flexible pavement design. The dependability of flexible pavement designs and subgrade strength variations are examined in this research. The average, maximum probability, median, & density distribution of subgrade strength are calculated. Both dependability and thickness of the design outputs are taken into consideration when using these procedures. In terms of dependability, the AASHTO technique outperforms the probabilistic approach. Finally, altering the HMA qualities are used to test the resiliency of the design of flexible pavement. To alleviate various problems, it is suggested that the present pavement thickness be modified by altering the material and subgrade qualities.

**Rahman et al (2011) [7]** Flexible pavement design often makes use of empirical methods like layered elastics and two-dimensional finite elements. More mechanical approaches are being used to lower the restrictions on stress, strain and displacement calculations for pavements nowadays. In order to achieve the study's requisite accuracy and convergence, researchers employed ABAQUS software to experiment with model size, element kinds, and meshing processes.

**Ameri et al (2012) [8]** Pavements have been studied and designed using FEA. it is possible to investigate stability, time-dependent issues, and material nonlinearity. The FEM and the Theory of Multilayer System have both been used to examine a large number of common pavements in this work. As a consequence of this statistical study, the significance parameter and correlation coefficient were used to compare the findings of these two methodologies. Finite-element analysis findings are best compared to those from the theory of multilayer systems in this research.

**Jain et al (2013) [9]** the design methodologies that have been historically used and the cost analysis for each type of rigid and flexible pavement design are discussed. Since

they can be reinforced and upgraded incrementally as traffic increases, flexible pavements outperform cement concrete roads in terms of durability. The initial investment and ongoing maintenance costs are lower with flexible pavement as well. Rigid pavement may be more expansive, but it requires less care and has a longer useful life. Flexible pavements have been shown to be more cost-effective for low-volume traffic. Flexible pavement has a life expectancy of around 15 years, however it requires regular maintenance after a given amount of time and the prices are quite expensive. More than 2.5 times as long as the 40-year life span of a flexible pavement.

**Dilip et.al (2013) [10]** In designing flexible pavements, consider the uncertainty associated with things like material qualities and traffic characterization. As a result of this, there have been major attempts in recent years to include dependability. The first- and second-order reliability methods, as well as a rudimentary Monte Carlo simulation, are used in this work to assess the resiliency of a flexible pavement segment. Narrow boundaries are also recommended.

**Maharaj and Gill (2014) [11]** used axisymmetric FEA to produce design charts by adjusting various parameters. Pressure and elastic modulus of the subgrade are variables that may change the thickness of pavement. Linear elastic material is idealized for pavement and base course and nonlinear material for subgrade by Drucker-Prager yield criteria. Four noded isoparametric finite element have been used to represent pavement, base course, and soil. We've come up with four different kinds of design charts. There are three criteria for each of the charts. The third set of parameters may be derived from the first two.

**Rezaei-Tarahomi et al. (2020) [12]** To properly estimate the maximum peak tensile stress of 156 different aircraft, they tried several multiple MLPNN topologies and training procedures. The intricacy of the challenges should be taken into account while calculating the size of the neural network.

**Kaya et al. (2018a) [13]** MLPNN-based dynamic modulus prediction models for hot and warm asphalt mixes were created, taking into account the gradation of aggregate, the characteristics of asphalt, and the volumetric properties.

Seitllari et al. (2019) [14] On an old asphalt mixture, we employed MLPNN with just one hidden layer to estimate the dynamic modulus shifts. HMA's dynamic modulus was similarly predicted using two-hidden-layer MLPNN models.

**Moghaddam et al. (2016) [15]** Neuronal networks may be used for fatigue life prediction by using MLPNN to estimate the fatigue life of asphalt mixtures containing polyethylene terephthalate.

**Tapkin (2014) [16]** The fatigue life of fly ash-modified thick asphalt mixes was predicted using MLPNNs with one, two, and three hidden layers. In order to take into consideration, the different methods of fatigue testing.

**Fakhri et al. (2017) [17]** Suggested a GA developed neural network for predicting the features of roller compacted concrete pavements. The GA was used in the training of the network. To further refine the effective amounts of cement, recovered asphalt pavement (RAP), and rubber, a sensitivity analysis was carried out as well.

**GA, Liu et al. (2020b) [18]** PVA fiber-reinforced cementitious composites, contain nano-SiO<sub>2</sub>, were produced using MLPNN compression strength prediction models and subsequently utilised to optimise composite mix proportions for compressive strength, as shown in this work (Fig. 1). In the development of the MLPNN, a GA-based optimization was used.

**Garoosiha et al. (2019) [19]** examined the concrete shrinkage prediction performance of MLPNNs with various designs and training procedures. There are a wide range of pavement materials that may benefit from MLPNN's non-linear representation of material performance vs composition. MLPNN, on the other hand, is prone to overfitting tiny experimental datasets.

**Dinegdae and Birgisson, 2018 [20]** In terms of truck traffic, autonomous vehicles immediately affect lane choice and lane arrangement. Automated (AV) trucks' lane selection and lane location are different from those controlled by humans (non-autonomous) vehicles. As a result, AVs will likely have a different impact on pavements than what is now the case. As a consequence of AVs-based systems' capacity to lane Centre and keep cars in a safe driving position, traffic will be channeled and heavy loads concentrated in a single narrow wheel path, resulting in congestion.

**Liu et al., 2019 [21]** Pavements are essential pieces of infrastructure that must be safeguarded. As a result, there is a pressing need to assess the potential effect of automated vehicles on roadways. In both the planning and building of new pavements and the maintenance of existing pavements, this applies. Existing pavement. structures

must be protected or maintained, and design approaches for future road constructions must be established using new sustainable procedures and materials.

**Xu (2017) [22]** designed the pavement in such a manner that the lateral wander is taken into account. Wheel position was predicted to follow a Laplace distribution on the transverse axis. It was him who determined the settings for the Dutch design method's broadband and dual tyre distribution characteristics. Strips of varying widths would be used to segment the lateral meandering. Afterwards, a correction factor was determined, that was defined as the difference in damage caused by lateral wandering and the damage that would occur if there was no wandering at all.

**Noorvand et al. (2017) [23]** The influence of autonomous trucks' lateral vehicle location on pavement infrastructure was examined. They devised a technique to ensure a uniform distribution of truck wheel wander. A random wheel wander was chosen as the reference case for the computed equivalency factors since it had a higher failure rate than the uniform or zero random wheel wander. Traffic was then calculated using these parameters as input.

**Chen et al. (2019) [24]** Each of these two-section uniform and two-section uniform lateral distributions has been plotted on a distribution curve. Analysis of wheel wander distributions & their impact on pavement structural behavior was done using a FE model.

**Gungor and Al-Qadi (2020) [25]** Autonomous and connected cars will benefit from a new pavement design framework dubbed Wander 2D. The goal was to figure out how much pavement degradation occurs when loads are applied laterally. To put it another way, the wheel wander is understood to be a shift in a function that reflects the specified damage metric. They provided a numerical illustration of the newly established approach inside the MEPDG damage frame.

**Zhou et al. (2019) [26]** They looked at the safety implications of AV wheel wander as well as the influence on fatigue and rutting performance in order to come up with recommendations on how to minimise AV's detrimental effect on pavement performance. All automobiles, autonomous or not, are thought to have a normal wheel wander distribution, according to their theory. In comparison to non-autonomous vehicles, autonomous automobiles had a wheel wander that was three times lower.

**Chen et al. (2019) [27]** Due to autonomous trucks' 0%-wheel wander, the requirement for pavement repair has been increased, according to this study. Autonomous truck wheel wander, on the other hand, has a positive impact on the rutting performance.

## CHAPTER 3

# RESEARCH GAP AND OBJECTIVES

### 3.1 Research Gap

All the previous researches were based on determining strength of different layers. But none of the researches were conducted on investigating the combined effect of each layer thickness on strength of pavement.

### 11 3.2 Objectives

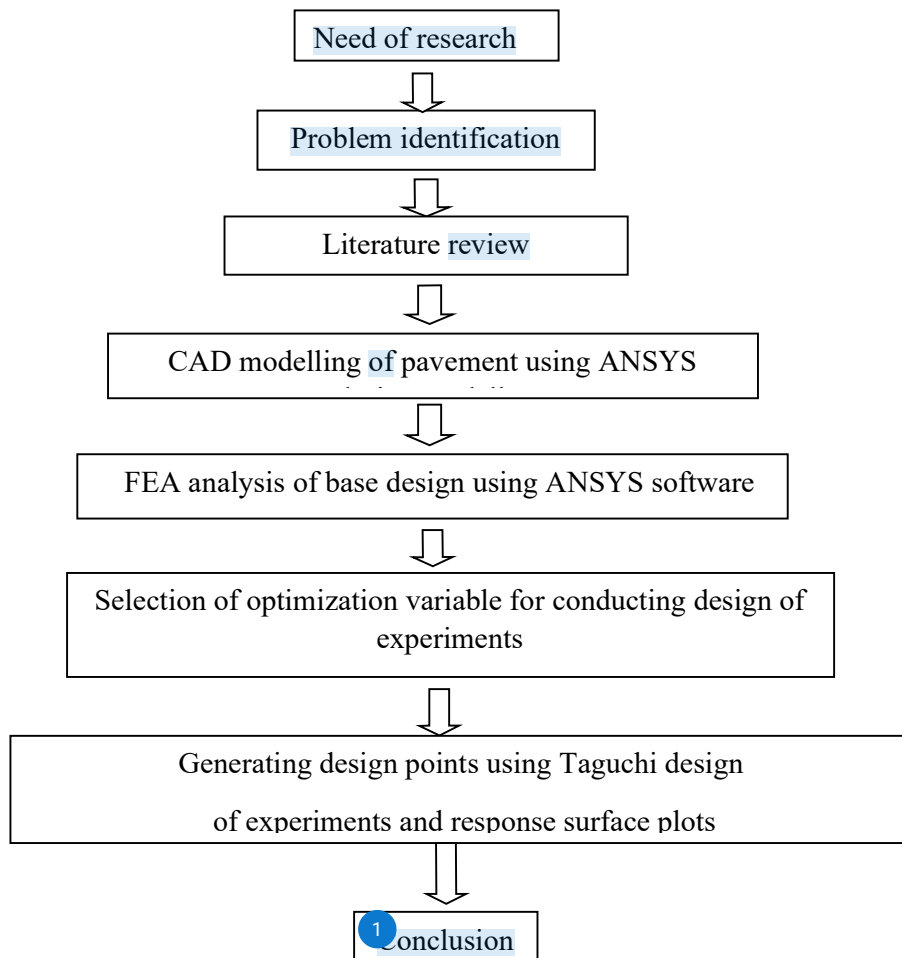
The objective of current research is to investigate the effect of pavement layer thickness on normal stress, shear stress, total deformation generated using Taguchi Response Surface optimization technique.

1. 2 CAD modeling of pavement using ANSYS design modeler software. Structural analysis on base design of pavement using ANSYS software.
2. Selection of optimization variables and conducting response surface optimization. These design points are width of different layers.
3. The DOE (design of experiments) table is generated and output parameters are evaluated for each design points generated. Generating sensitivity plot, 3d response surface plot and 2D response surface plot to aid in understanding the effect of each design variable.

## 11 CHAPTER 4

# METHODOLOGY

## 4.1 Methodology



## 4.2 Methodology Steps

The analysis of pavement is conducted using techniques of FEM. Different stages of FEM are discussed in this section.

### 4.2.1 CAD Modelling

The CAD model of pavement developed in ANSYS design modeler as given in figure 4.1 below.

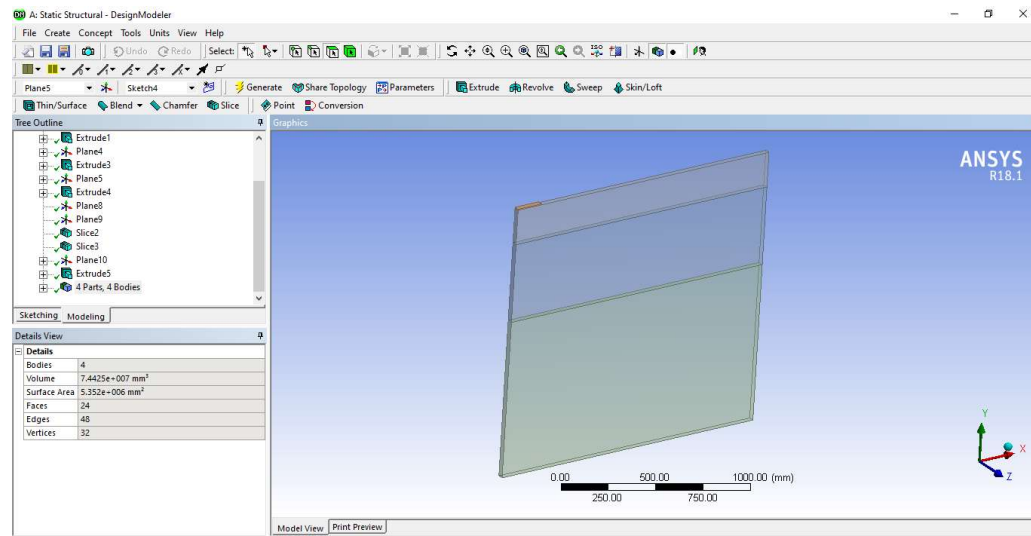


Figure 4.1: CAD model of pavement

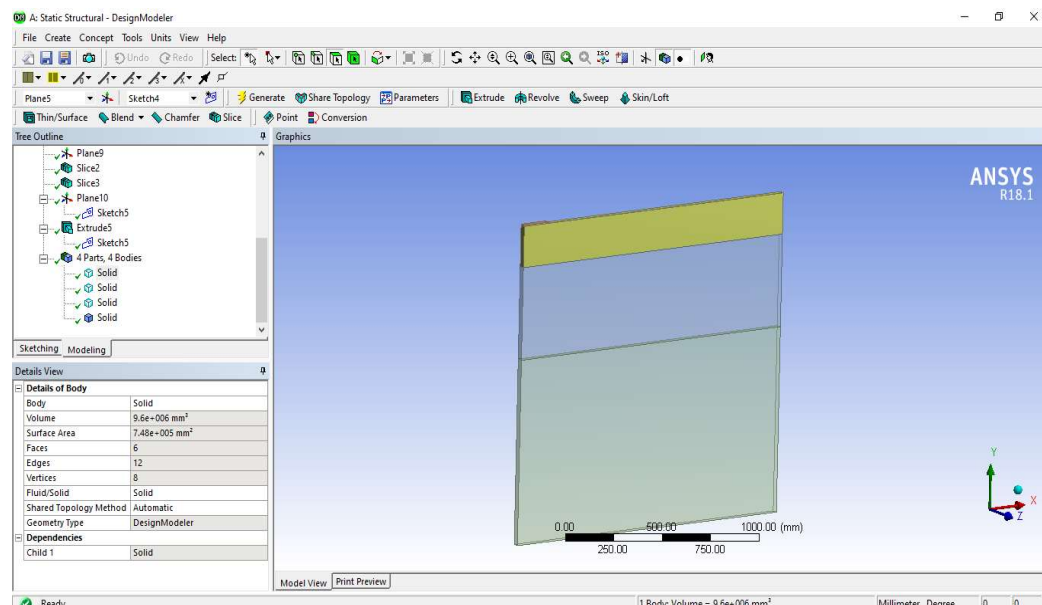


Figure 4.2: CAD model of pavement



The layer highlighted in figure 4.2 above comprises of <sup>40</sup> wearing course and binder course. The next layer is given in figure 4.3 below which is base layer and sub base layer.

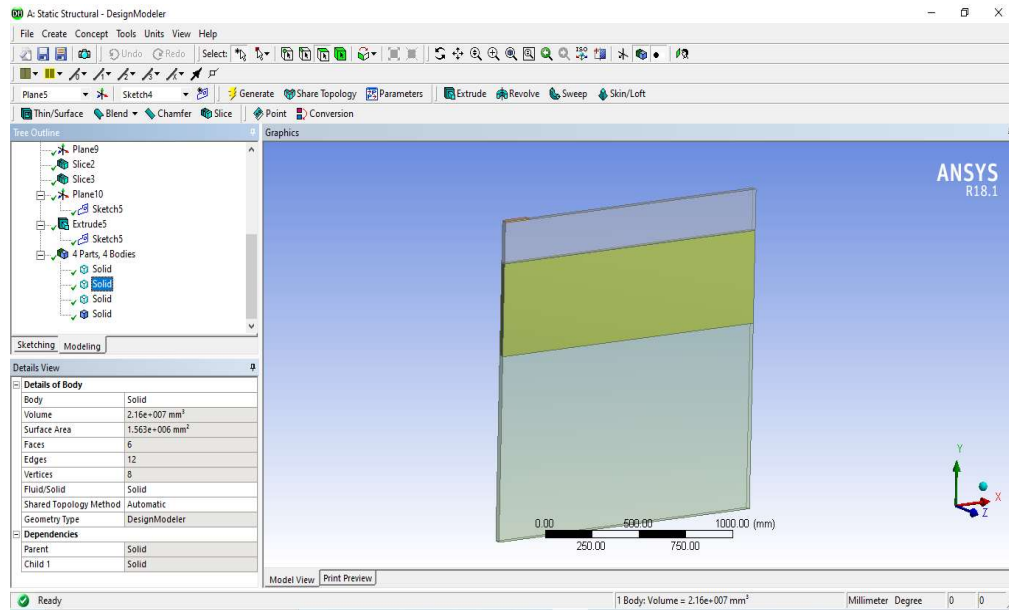


Figure 4.3: CAD model of pavement base layer

The bottommost layer of pavement is subgrade layer as <sup>32</sup> given in figure 4.4 below.

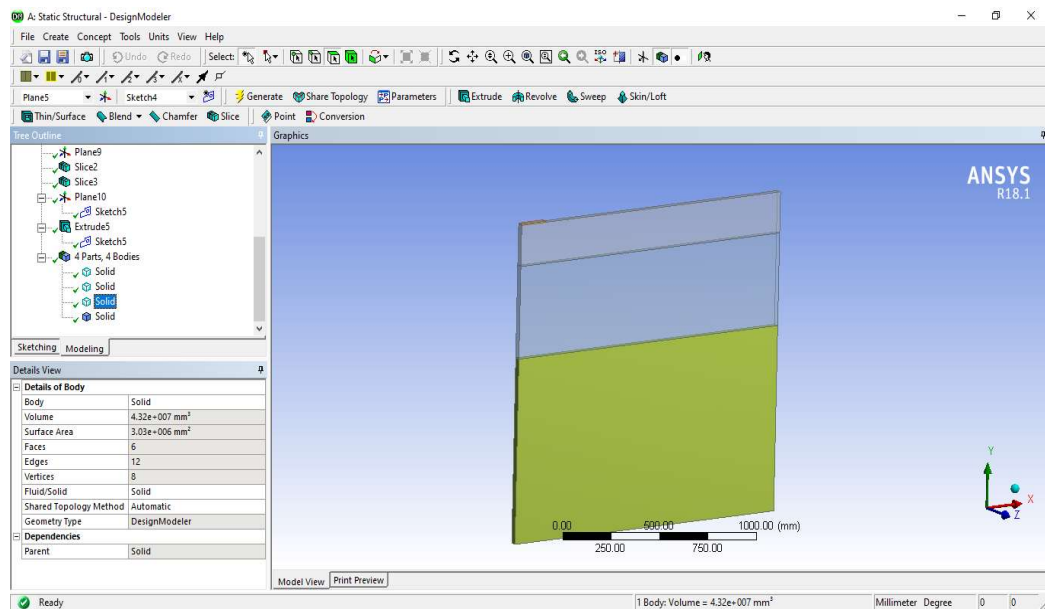


Figure 4.4: CAD model of pavement subgrade

### 13 4.2.2 Meshing CAD Modelling in ANSYS

After CAD design of pavement is developed, it is meshed using hexahedral elements. The 12 number of elements generated is 296 and number of nodes generated is 2469. Due to topological consistency the model is suited for hexahedral elements.

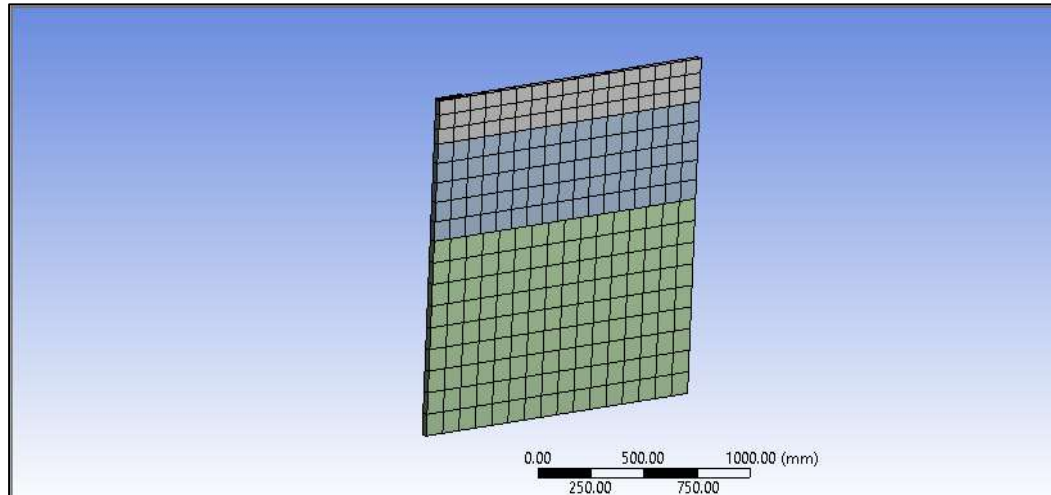
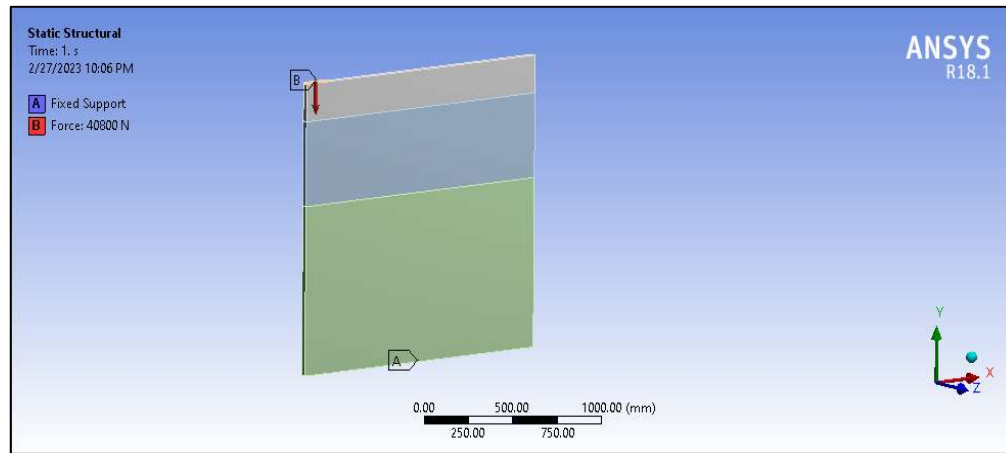


Figure 4.5: Hexahedral element meshed

### 1 4.2.3 Applying Loads and Boundary Conditions

As seen in above picture, the CAD model is used in conjunction with the proper loads and boundary conditions, which support both force and displacement. According to published research, loads and boundary conditions are applied. Pavement bases are applied with fixed support. The loading condition are applied as per Indian Road Congress (IRC: 37-2012).



8 Figure 4.6: Loads and boundary condition

## 4.2.4 Solution Stage

For each type of element, the stiffness matrix is now created. For deformation and stresses, nodal computations are performed. These outcomes interpolate for the edge length of the entire element.

## 4.2.5 Response Surface Methodology for Design Optimization

A "set of mathematical and statistical techniques that are useful for analyzing problems in which several independent variables affect a dependent variable or response" [28] is known as the response surface method (RSM). Optimizing this response is the main objective. We assume that these variables, which represent the independent variables  $X_1$ ,  $X_2$ ,  $X_3$ ,  $X_4$ , and so forth, are continuous and that the researcher can manipulate them with little error [29]. Following is a representation of how the dependent variable and independent variable are related

$$9 \quad y = f(X_1, X_2, X_3, X_4, \dots, X_n) + \varepsilon$$

where  $\varepsilon$  represents the noise or error observed in the "y" response.

If we denote the expected answer with

$$E(y) = f(X_1, X_2, X_3, X_4, \dots, X_n) = \eta$$

then, the surface represented by

$$f(X_1, X_2, X_3, X_4, \dots, X_n) = \eta$$

is called the response surface[29].

The optimization parameters selected for optimization are given in table 4.1 below.

Table 4.1: Optimization variables

Subgrade	900mm
Baselayer	450mm
Bl	200mm

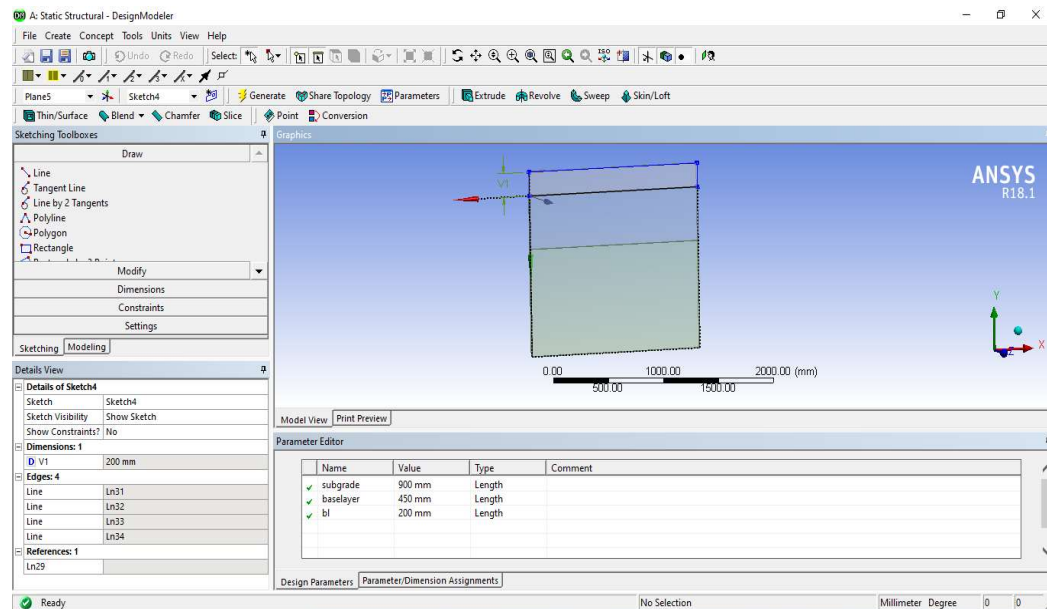


Figure 4.7: Variable definition for optimization

## CHAPTER 5

## RESULT AND DISCUSSION

### 5.1 FEA Results on Pavement

The FE analysis is conducted on pavement to determine normal stresses. The maximum normal stress along horizontal direction is observed to be 6.6653MPa shown in red colored region. The normal stress is maximum at the point of load application which reduces along the downward direction.

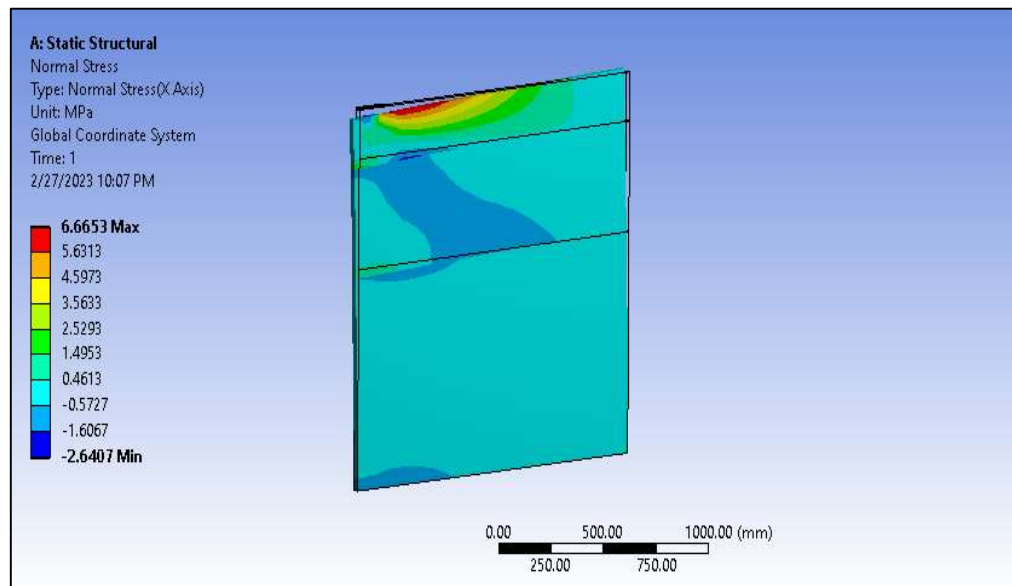


Figure 5.1: Maximum normal stress along x direction (horizontal direction)

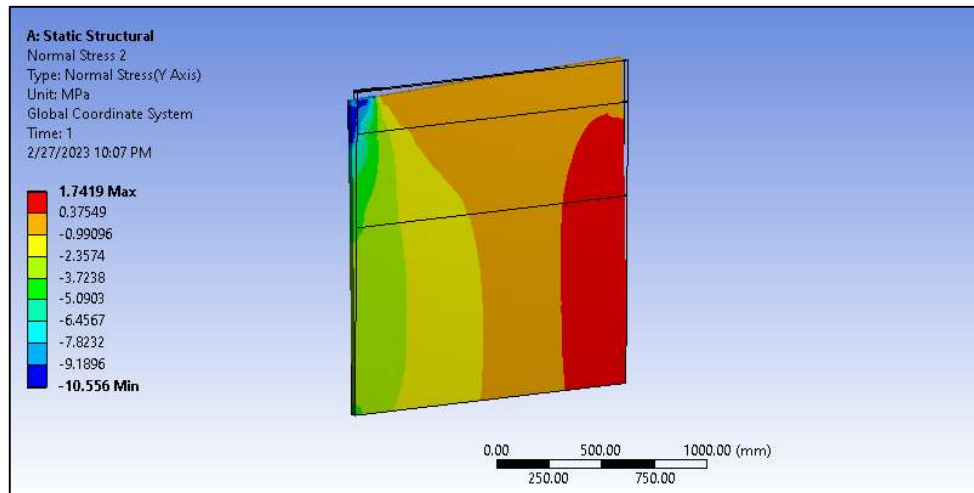


Figure 5.2: Maximum normal stress along y direction (vertical direction)

The maximum normal stress along the vertical direction is given in figure 5.2 above. The maximum normal stress is observed at the zone of load application with magnitude of 10.55MPa as shown in dark blue colored zone. The normal stress reduces as we move towards the bottom region of pavement.

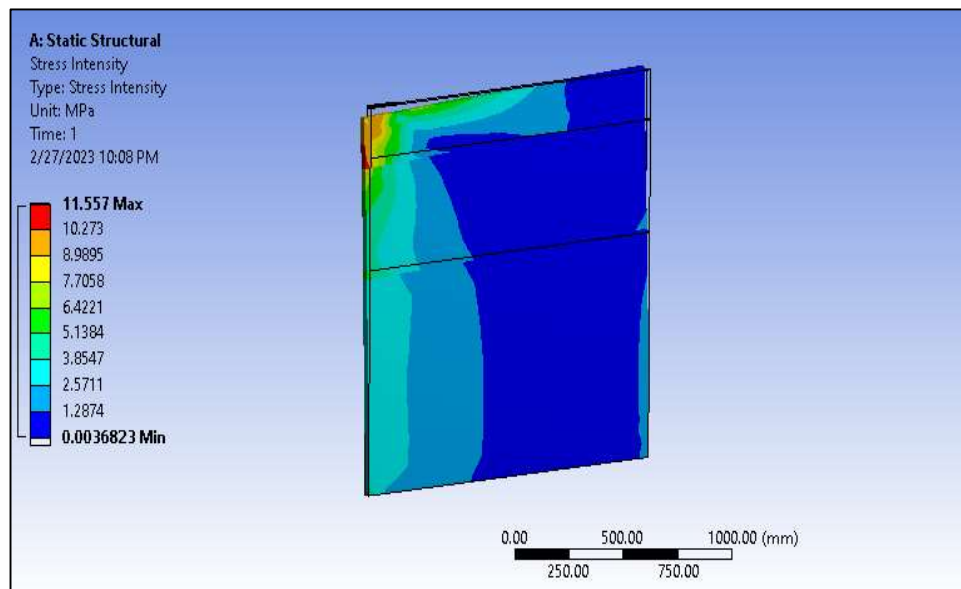


Figure 5.3: Maximum normal stress intensity

The normal stress intensity plot is obtained from the FEA analysis of pavement. The maximum stress intensity is obtained at the corner region with magnitude of 11.557MPa which reduces towards the bottom region and at the other free end.

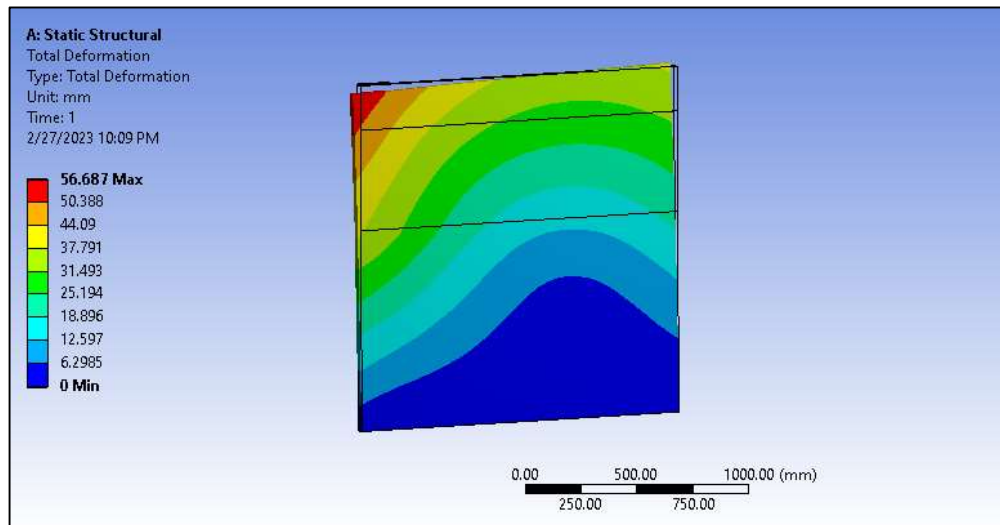


Figure 5.4: Total deformation plot

The total deformation plot is obtained from the FEA and the maximum deformation obtained from the FEA is 56.687mm at the point of load application which reduces towards the base of pavement and at the free end of pavement.

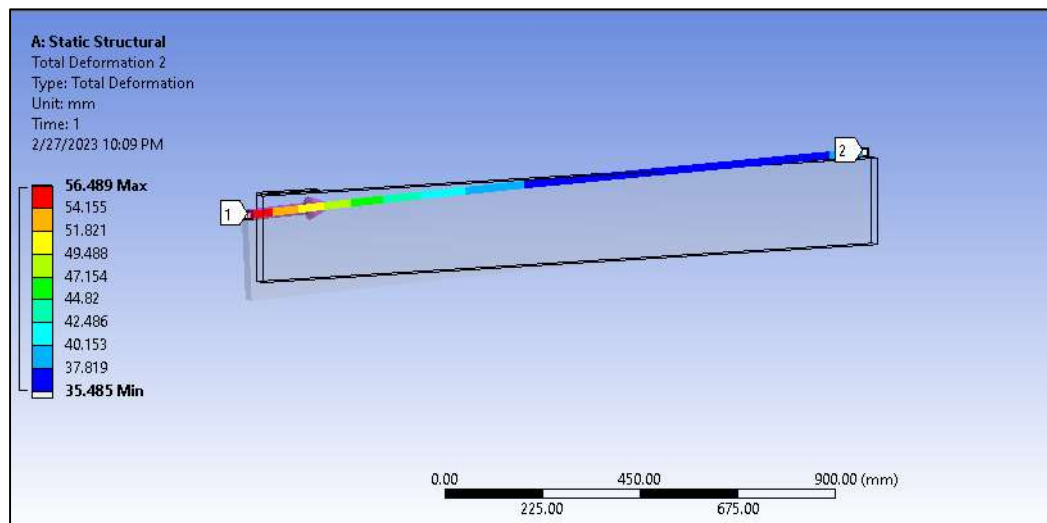


Figure 5.5: Total deformation plot across length

The variation of total deformation along the length of pavement is given in figure 5.5 above. The total deformation is maximum at the zone of load application.

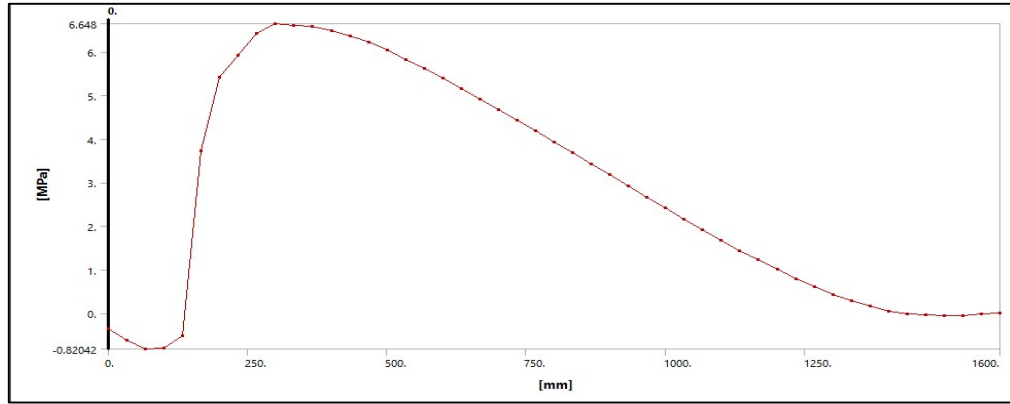


Figure 5.6: Normal stress along the length

The variation of normal stress along the length is given in figure 5.6 above. The normal stress increases and reaches to max with magnitude of 6.648MPa and reduces linearly thereafter. The graph is similar to given in literature [30].

## 5.2 Response Surface Optimization

The DOE table is generated from taguchi response surface optimization method. It includes optimization variables i.e. subgrade, base layer and bl. The output parameters include normal shear stress, normal stress, total deformation. The design points are generated using linear regression model.

	A	B	C	D	E	F	G
1	Name	P4 - subgrade (mm)	P5 - baselayer (mm)	P6 - bl (mm)	P1 - Shear Stress Maximum (MPa)	P2 - Normal Stress 2 Maximum (MPa)	P3 - Total Deformation Maximum (mm)
2	1	900	450	200	0.072208	1.7419	56.687
3	2	810	450	200	0.085802	1.7838	55.707
4	3	990	450	200	0.069845	1.7277	58.23
5	4	900	405	200	0.072998	1.7501	56.109
6	5	900	495	200	0.070672	1.7344	57.403
7	6	900	450	180	0.072261	1.7455	56.408
8	7	900	450	220	0.07122	1.7385	56.99
9	8	826.83	413.41	183.74	0.057271	1.7922	55.601
10	9	973.17	413.41	183.74	0.071213	1.7385	56.995
11	10	826.83	486.59	183.74	0.073263	1.7516	56.025
12	11	973.17	486.59	183.74	0.069789	1.7272	58.299
13	12	826.83	413.41	216.26	0.088201	1.7845	55.686
14	13	973.17	413.41	216.26	0.070514	1.7332	57.54
15	14	826.83	486.59	216.26	0.07227	1.7455	56.404
16	15	973.17	486.59	216.26	0.06931	1.7228	58.962

Figure 5.7: DOE table generated



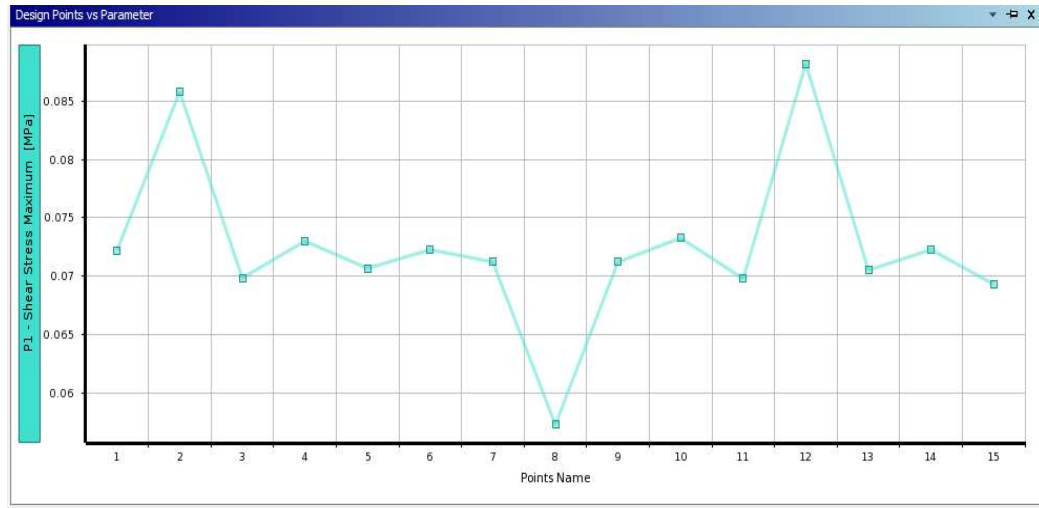


Figure 5.8: Shear stress vs design points

As its evident from <sup>8</sup>figure 5.8 above, the minimum shear stress is obtained for design point number 8 which has dimensions of 826.83mm subgrade and 413.41 base layer and 183.74mm bl.

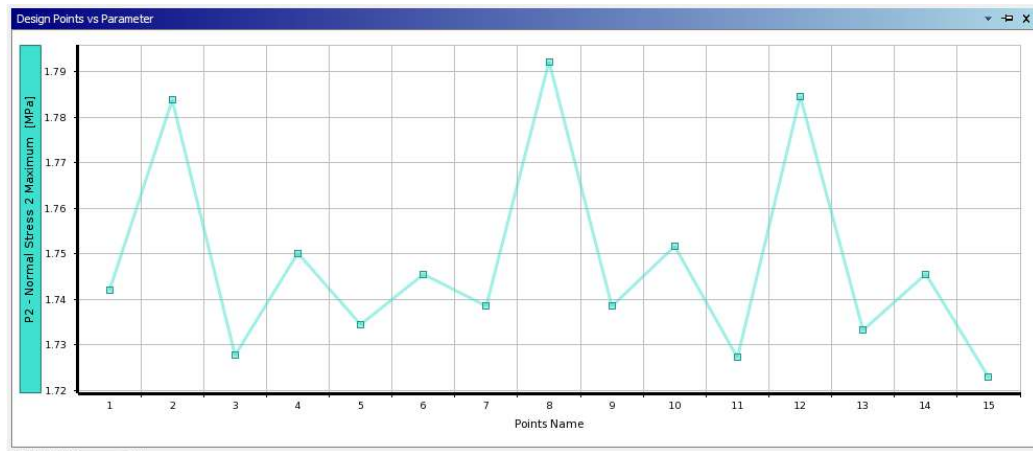


Figure 5.9: Normal stress vs design points

As its evident from <sup>8</sup>figure 5.9 above, the minimum normal stress is obtained for design point number 15 which has dimensions of 973.17mm subgrade and 486.59mm base layer and 216.26mm bl.

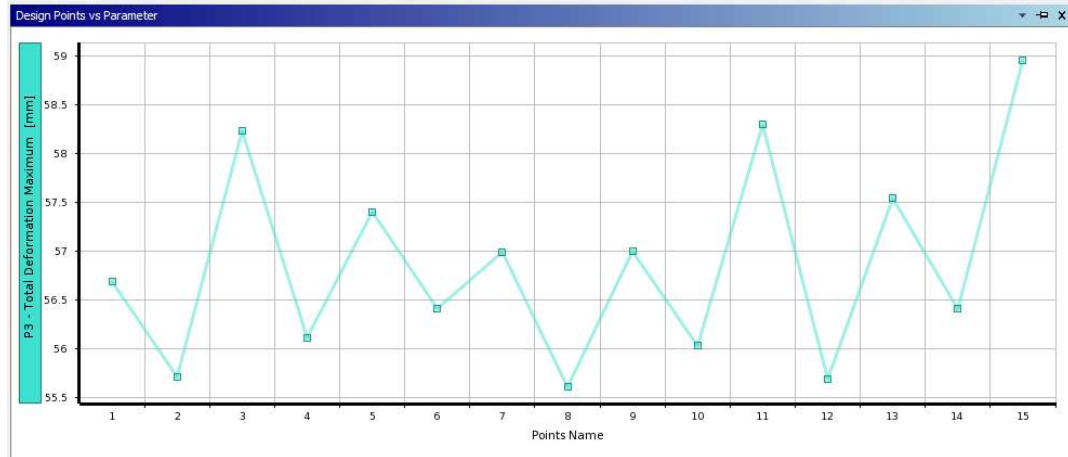


Figure 5.10: Total deformation vs design points

As its evident from figure 5.10 above, the minimum total deformation is obtained for design point number 8 which has dimensions of 826.83mm subgrade and 413.41 base layer and 183.74mm and maximum deformation is observed for design point number 15

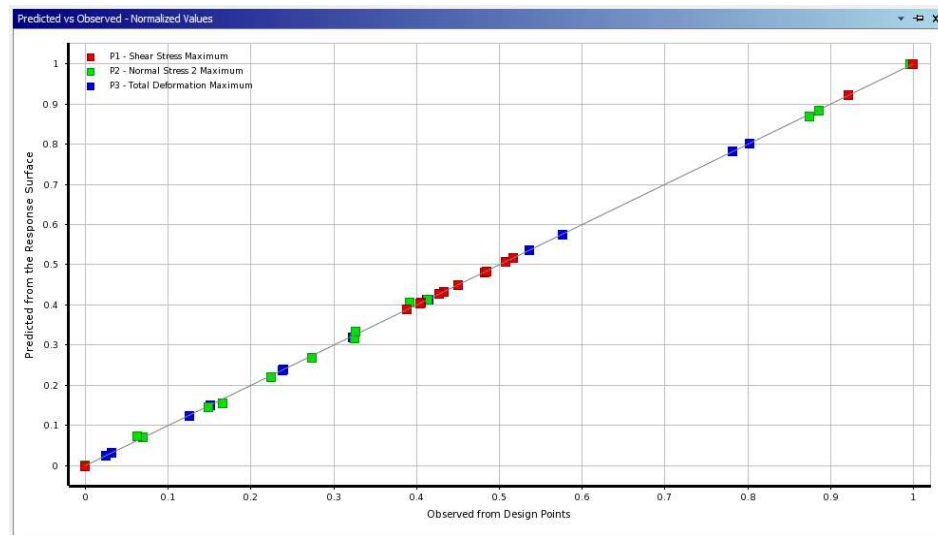


Figure 5.11: Goodness of fit curve

The goodness of fit curve is obtained from solution which shows the exactness of the DOE solution. From the current solution it is evident that very little deviation is observed for obtained values (represented in boxes) as compared to expected values (as represented in line).

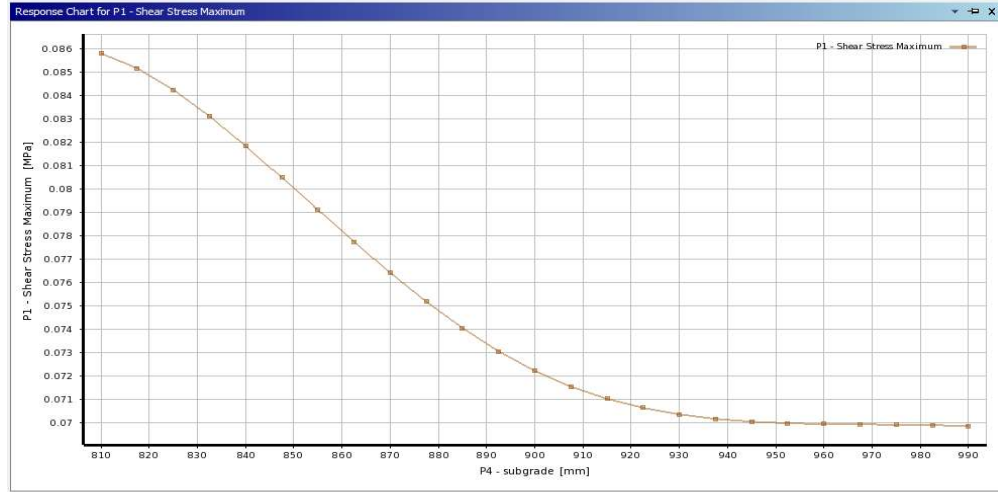


Figure 5.12: Shear stress vs subgrade

The variation of shear stress with respect to subgrade is given in figure 5.12. The shear stress decreases gradually with increase in subgrade layer and reaches to almost constant stage after 940mm of subgrade thickness. The maximum shear stress was observed for 810mm subgrade thickness value.

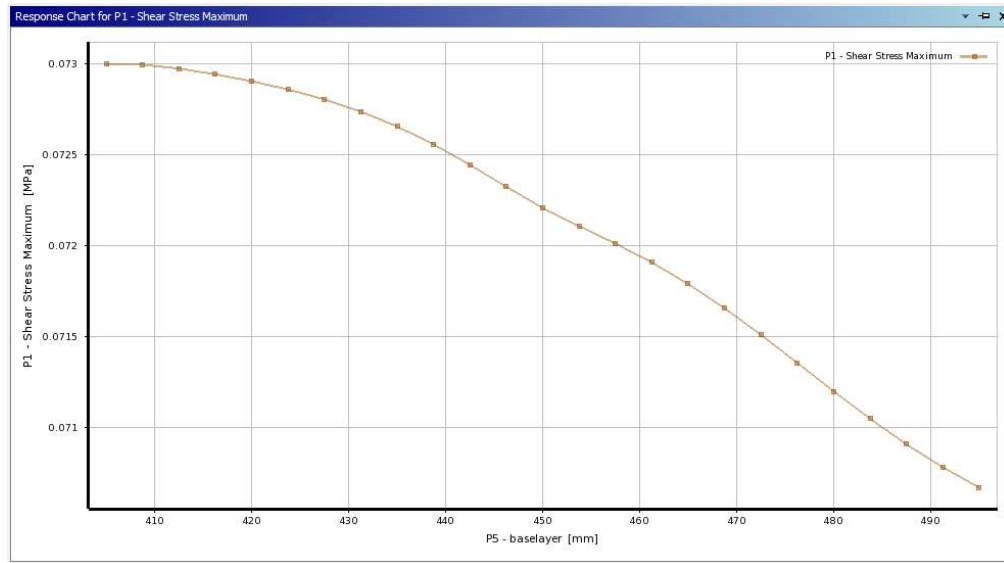


Figure 5.13: Shear stress vs baselayer

The variation of shear stress with respect to baselayer is given in figure 5.13. The shear stress decreases gradually with increase in base layer thickness and reaches to minimum value at 495mm of baselayer thickness. The maximum shear stress was observed for 405mm baselayer thickness value.

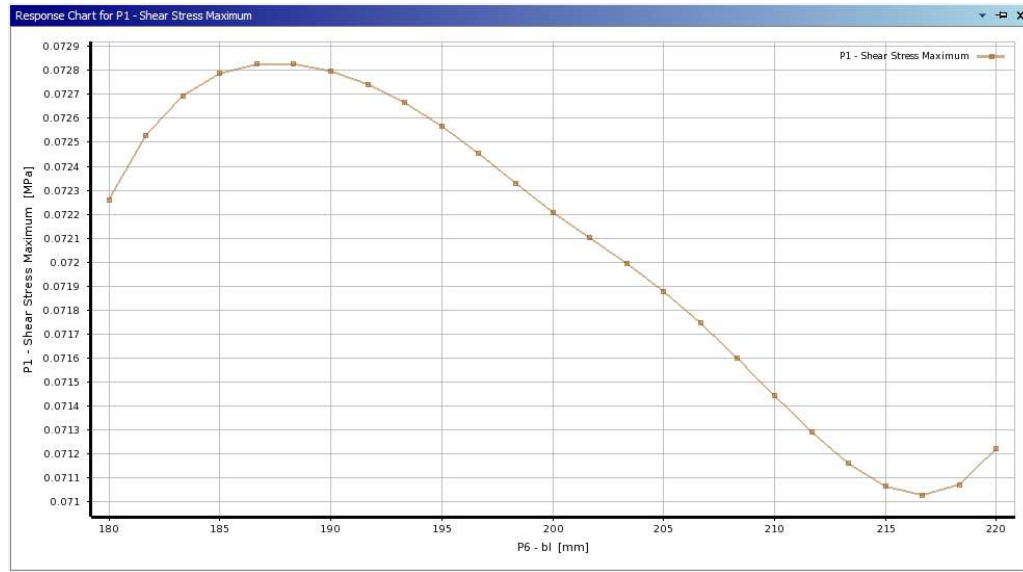


Figure 5.14: Shear stress vs bl

The variation of shear stress with respect to bl is given in figure 5.14. The shear stress initially increases to reach maximum value at 186mm bl and then decreases linearly thereafter to reach minimum value at 216mm bl.

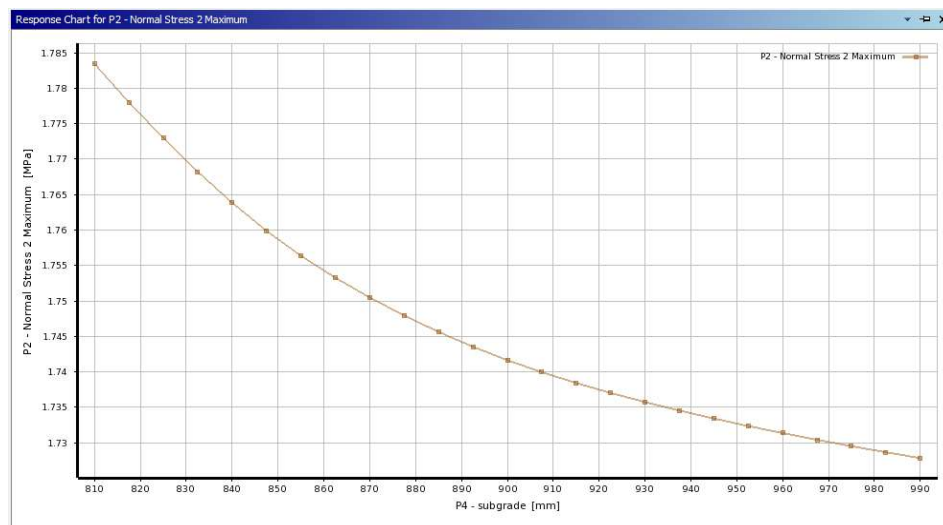


Figure 5.15: Normal stress vs subgrade

The variation of normal stress with respect to subgrade is given in figure 5.15. The shear normal decreases gradually with increase in subgrade layer and reach to almost constant stage after 990mm of subgrade thickness. The maximum normal stress was observed for 810mm subgrade thickness value.

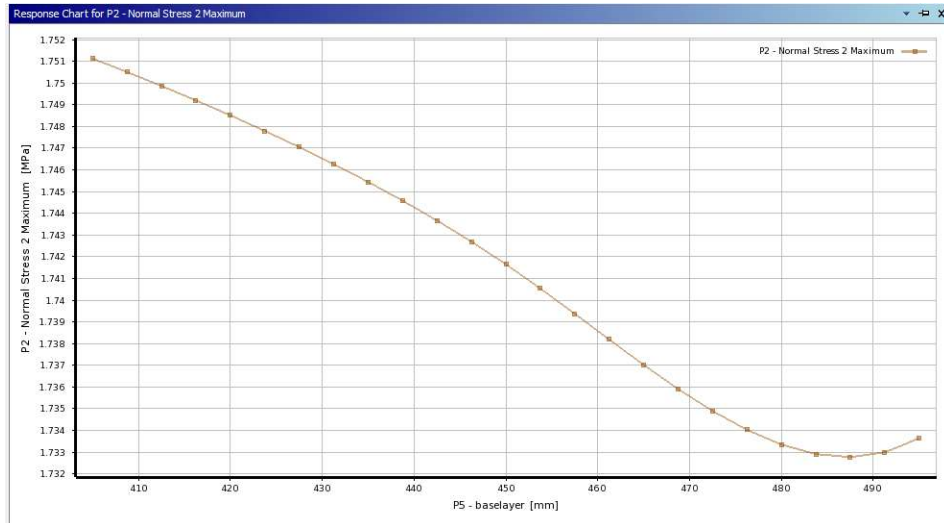


Figure 5.16: Normal Stress vs baselayer

The variation of normal stress with respect to baselayer is given in figure 5.16. The normal stress decreases gradually with increase in base layer thickness and reaches to minimum value at 485mm of baselayer thickness.

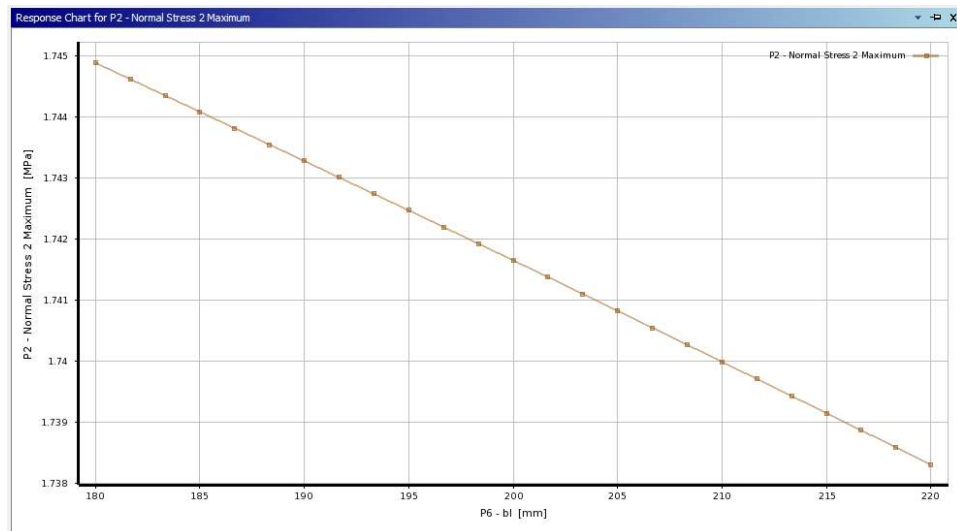


Figure 5.17: Normal Stress vs bl

The variation of normal stress with respect to bl is given in figure 5.17. The normal stress linearly decreases with increase in bl value and reaches to minimum value at 220mm. The maximum normal stress was observed for bl value of 180mm.

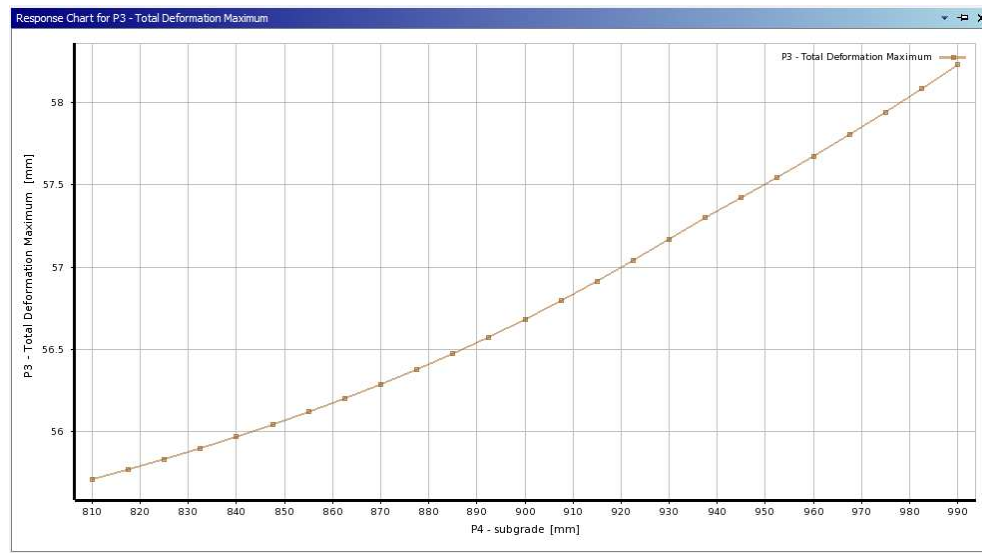


Figure 5.18: Total deformation vs subgrade

The variation of total deformation with respect to subgrade is given in figure 5.18. The total deformation increases exponentially with increase in subgrade value. The minimum total deformation is observed for subgrade value of 810mm and maximum total deformation is observed for subgrade value of 990mm.

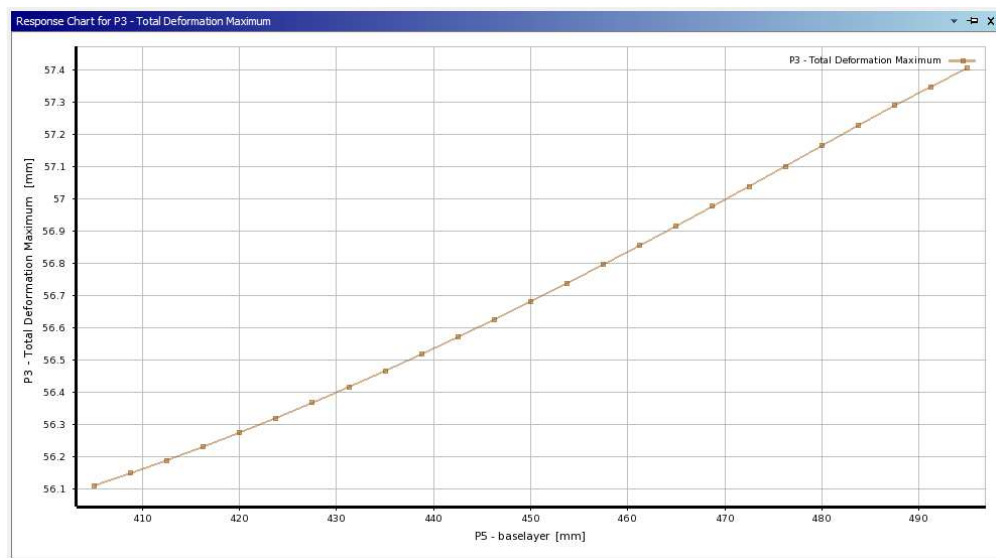


Figure 5.19: Total deformation vs baselayer

The variation of total deformation with respect to baselayer is given in figure 5.19. The total deformation increases exponentially with increase in baselayer value. The minimum total deformation is observed for baselayer value of 405mm and maximum total deformation is observed for baselayer value of 495mm.

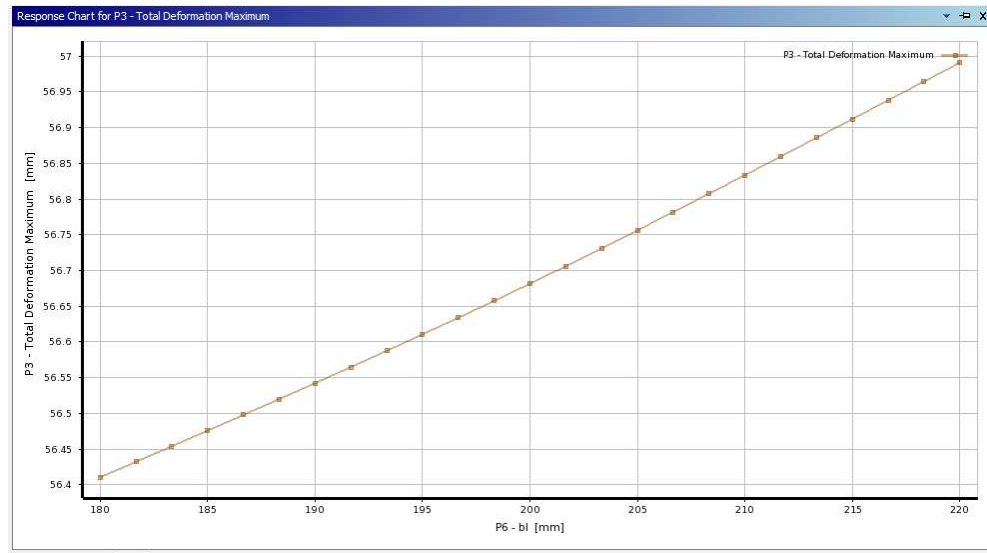


Figure 5.20: Total deformation vs bl

The variation of total deformation with respect to bl is given in figure 5.20. The total deformation increases exponentially with increase in bl value. The minimum total deformation is observed for bl value of 180mm and maximum total deformation is observed for bl value of 220mm.

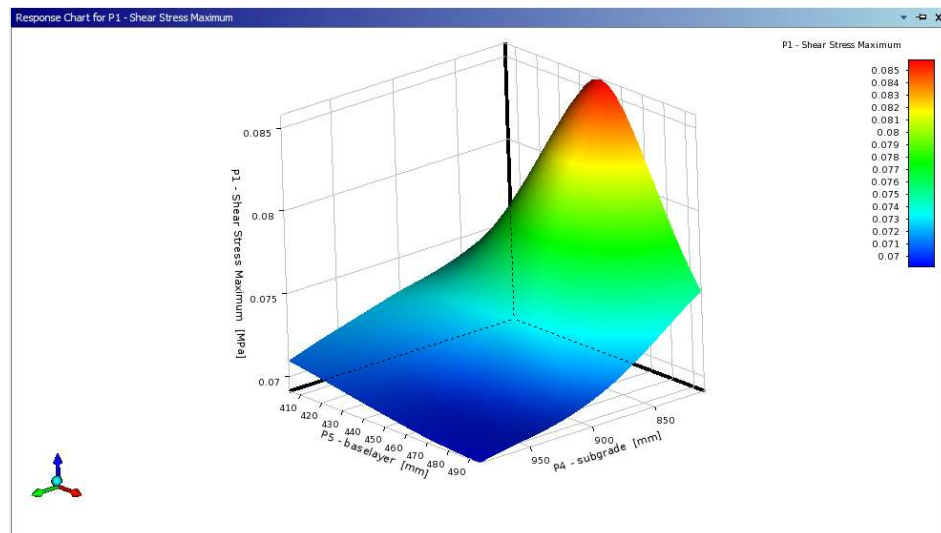


Figure 5.21: Response surface plot of shear stress

The variation of response surface plot of shear stress is given in figure 5.21 above. The shear stress is maximum for subgrade value ranging from 800mm to 850mm and baselayer value ranging from 420mm to 470mm value. The shear stress is minimum for regions shown in dark blue colored region.

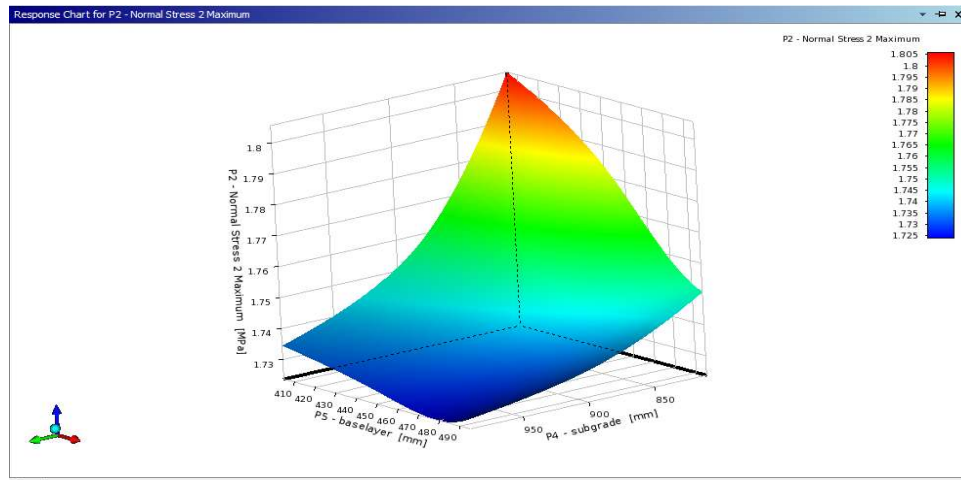


Figure 5.22: Response surface plot of normal stress

The 3D response surface plot normal stress is given in figure 5.22 above. The maximum normal stress on pavement is observed for subgrade value ranging from 800mm to 825mm and baselayer value ranging from 410mm to 440mm. The normal stress minimum for regions shown in dark blue colored zone.

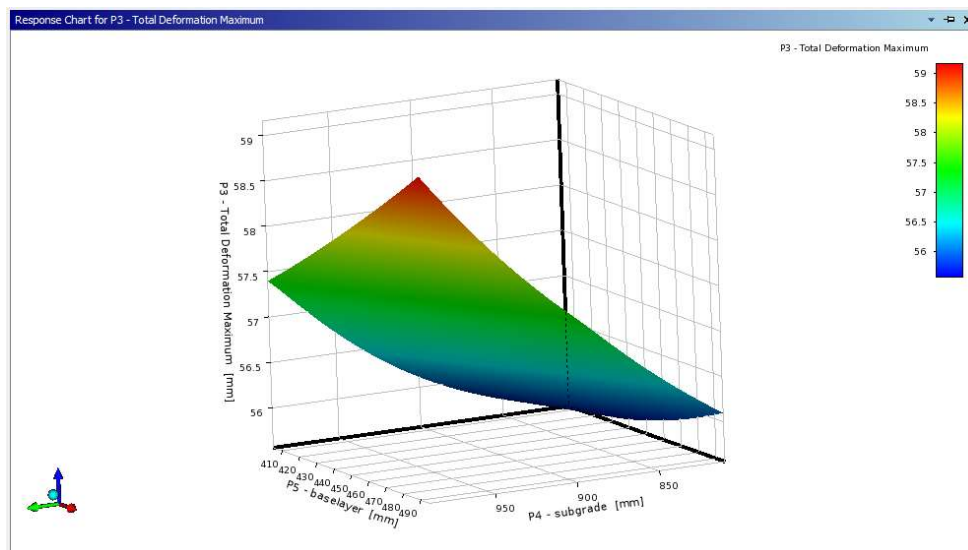


Figure 5.23: Response surface plot of total deformation

The 3D response surface plot of total deformation is given in figure 5.23 above. The maximum total deformation on pavement is observed for subgrade value higher than 950mm and baselayer value ranging from 460mm to 490mm. The total deformation is minimum for regions shown in dark blue colored zone.



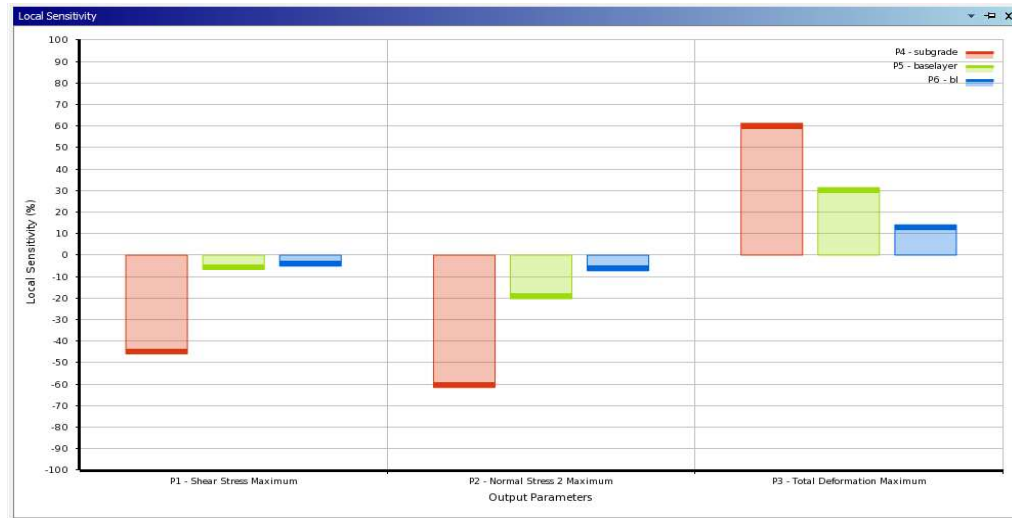


Figure 5.24: Sensitivity percentage plot

The sensitivity plots are generated for different variables and output parameters. For shear stress, the bl layer thickness has lowest sensitivity percentage of 5.1185% whereas the subgrade layer has highest sensitivity percentage of 45.926% and base layer has sensitivity percentage of 6.6943%. The higher sensitivity percentage of subgrade layer shows that subgrade layer thickness has highest effect on shear stress.

For normal stress, the bl layer thickness has lowest sensitivity percentage of 7.2871% whereas the subgrade layer has highest sensitivity percentage of 61.553% and base layer has sensitivity percentage of 20.267%. The higher sensitivity percentage of subgrade layer shows that subgrade layer thickness has highest effect on normal stress.

2 For total deformation, the bl layer thickness has lowest sensitivity percentage of 14.1% whereas the subgrade layer has highest sensitivity percentage of 61.293% and base layer has sensitivity percentage of 31.435%. The higher sensitivity percentage of subgrade layer shows that subgrade layer thickness has highest effect on total deformation.

## <sup>1</sup>CHAPTER 6

# CONCLUSION AND FUTURE SCOPE

## 6.1 Conclusion

The FEA analysis is conducted on pavement<sup>36</sup> to determine the effect of single wheel load on flexible pavement. From the FEA analysis, critical regions of pavement having high normal stress, deformation on flexible pavement is determined. The effect of different pavement layer thickness is then analysed using Taguchi response and the findings are summarized below.

- <sup>43</sup>1. The minimum shear stress is obtained for design which has dimensions of 826.83mm subgrade and 413.41 base layer and 183.74mm bl.
2. The minimum normal stress is obtained for design which has dimensions of 973.17mm subgrade and 486.59mm base layer and 216.26mm bl.
3. The minimum total deformation is obtained for which has dimensions of 826.83mm subgrade and 413.41 base layer and 183.74mm bl.
4. For shear stress, the higher sensitivity percentage of subgrade layer shows that subgrade layer thickness has highest effect on shear stress.
5. For normal stress, the higher sensitivity percentage of subgrade layer shows that subgrade layer thickness has highest effect on normal stress.
6. For total deformation, the higher sensitivity percentage of subgrade layer shows that subgrade layer thickness has highest effect on deformation.

## **6.2 Future Scope**

Further analysis can be conducted on pavement by changing material of different layers. The material properties of these layers especially stiffness has significant effect on deformation and normal stress. The use of replacement materials like coal dust, brick dust, replacement aggregates.

## REFERENCE

1. Considerations of Bituminous Pavement Design by Mechanistic-Empirical Approach, the International Journal of Pavement Engineering, Vol.9, No.1, pp. 19-31.
2. Tarefder, R., Saha, N. and Stormont, J.(2010) Evaluation of Subgrade Strength and Pavement Designs for Reliability, Journal Transportation Engineering, Vol.136, No.4, pp. 379-391.
3. Rahman, M.T., Mahmud, K. and Ahsan, K. (2011), Stress-Strain Characteristics of Flexible Pavement Using Finite Element Analysis, International Journal of Civil and Structural Engineering, Vol.2, No.1, pp.233-240.
4. Ameri, M., Salehabadi, E.G., Nejad, F.M. and Rostami, T. (2012) Assessment of Analytical Techniques of Flexible Pavements by Finite Element Method and Theory of Multi-Layer System, Journal Basic Applied Science Research, Vol.2, No.11, pp.11743-11748.
5. Jain, S., Joshi, Y.P., Golia, S.S. (2013) Design of Rigid and Flexible Pavements by Various Methods and Their Cost Analysis of Each Method, International Journal of Engineering Research and Applications, Vol.3, No.5 pp.119-123.
6. Dilip, D., Ravi, P. and Babu, G. (2013) System Reliability Analysis of Flexible Pavements, Journal Transportation Engineering, Vol.139, No.10, pp. 1001-1009.
7. Maharaj, D.K. and Gill, S. (2014) Development of Design Chart for Flexible Pavement by Finite Element Method, International Journal of Latest Research in Engineering and Computing, Vol.2, Issue 2, MarchApril, pp.8-23.
8. Rezaei-Tarahomi, A., Ceylan, H., Gopalakrishnan, K., et al., 2019. Artificial neural network models for airport rigid pavement top-down critical stress

predictions: sensitivity evaluation. In: International Airfield and Highway Pavements Conference 2019, Chicago, 2019.

9. Kaya, O., Rezaei-Tarahomi, A., Ceylan, H., et al., 2018b. Neural network-based multiple-slab response models for top-down cracking mode in airfield pavement design. Journal Khan, I.H. (1998) A Textbook of Geotechnical Engineering, Pentice Hall of India Private Limited, New Delhi.
10. Arora, K.R. (2003) Soil mechanics and Foundation Engineering, Standard Publishers Distributors, Delhi
11. Punmia, B.C., Jain, A.K. and Jain Arun, K. (2005) Soil Mechanics and Foundations, Lakshmi Publications, New Delhi.
12. Subagio, B. Cahyanto, H., Rahman, A. and Mardiyah, S. (2005) Multilayer Pavement Structural Analysis Using Method of Equivalent Thickness, Case Study: Jakarta-Cikampek Toll Road , Journal of the Eastern Asia Society for Transportation Studies, Vol.6,pp.55-65.
13. Das, A. (2008) Reliability of Transportation Engineering, Part B: Pavements 144 (2), 04018009
14. Seitllari, A., Kumbarger, Y.S., Biligiri, K.P., et al., 2019. A soft computing approach to predict and evaluate asphalt mixture aging characteristics using asphaltene as a performance indicator. Materials and Structures 52, 100.
15. Moghaddam, T.B., Soltani, M., Shahraki, H.S., et al., 2016. The use of SVM-FFA in estimating fatigue life of polyethylene terephthalate modified asphalt mixtures. Measurement 90, 526e533.
16. Tapkin, S., 2014. Estimation of fatigue lives of fly ash modified dense bituminous mixtures based on artificial neural networks. Materials Research 17 (2), 316e325.

17. Fakhri, M., Amoosoltani, E., Farhani, M., et al., 2017. Determining optimal combination of roller compacted concrete pavement mixture containing recycled asphalt pavement and crumb rubber using hybrid artificial neural network-genetic algorithm method considering energy absorbency approach. *Canadian Journal of Civil Engineering* 44 (11), 945e955.
18. Liu, T., Zhang, P., Wang, J., et al., 2020b. Compressive strength prediction of PVA fiber-reinforced cementitious composites containing nano-SiO<sub>2</sub> using BP neural network. *Materials* 13 (3), 521.
19. Garoosiha, H., Ahmadi, J., Bayat, H., et al., 2019. The assessment of Levenberg-Marquardt and Bayesian framework training algorithm for prediction of concrete shrinkage by the artificial neural network. *Cogent Engineering* 6 (1), 1609179.
20. Dinegdae, Y.H., Birgisson, B., 2018. Effects of truck traffic on topdown fatigue cracking performance of flexible pavements using a new mechanics-based analysis framework. *Road Materials and Pavement Design* 19 (1), 182e200.
21. Liu, Y., Tight, M., Sun, Q., et al., 2019. A systematic review: road infrastructure requirement for connected and autonomous vehicles (CAVs). *Journal of Physics: Conference Series* 1187 (4), 42e73.
22. Xu, Q., 2017. A Potential New Structural Design for Flexible Pavement (Master thesis). Delft University of Technology, Delft.
23. Noorvand, H., Karnati, G., Underwood, B.S., 2017. Autonomous vehicles: assessment of the implications of truck positioning on flexible pavement performance and design. *Transportation Research Record* 2640, 21e28.
24. Chen, F., Song, M., Ma, X., et al., 2019. Assess the impacts of different autonomous trucks' lateral control modes on asphalt pavement performance. *Transportation Research Part C: Emerging Technologies* 103, 17e29.

25. Gungor, O.E., Al-Qadi, I.L., 2020. Wander 2D: a flexible pavement design framework for autonomous and connected trucks. *International Journal of Pavement Engineering*, <https://doi.org/10.1080/10298436.2020.1735636>.
26. Zhou, F., Hu, S., Xue, W., et al., 2019. Optimizing the Lateral Wandering of Automated Vehicles to Improve Roadway Safety and Pavement Life. Final Report. Texas A&M Transportation Institute, College Station.
27. Chen, F., Song, M., Ma, X., et al., 2019. Assess the impacts of different autonomous trucks' lateral control modes on asphalt pavement performance. *Transportation Research Part C: Emerging Technologies* 103, 17e29.
28. M. Avallé, G. Chiandussi, and G. Belingardi, "Design optimization by response surface methodology: application to crashworthiness design of vehicle structures," *Struct. Multidiscip. Optim.*, vol. 24, no. 4, pp. 325–332, 2002, doi: 10.1007/s00158-002-0243-x.
29. Y. A. E.-V. Silva, "Utilization of Response Surface Methodology in Optimization of Extraction of Plant Materials," Rijeka: IntechOpen, 2018, p. Ch. 10.
30. M.S. Ranadive, Anand B. Tapase, "Parameter sensitive analysis of flexible pavement" *International Journal of Pavement Research and Technology* 9 (2016) 466–472

## 17% Overall Similarity

Top sources found in the following databases:

- 8% Internet database
- Crossref database
- 16% Submitted Works database
- 6% Publications database
- Crossref Posted Content database

### TOP SOURCES

The sources with the highest number of matches within the submission. Overlapping sources will not be displayed.

1	<b>University of Bolton on 2022-05-15</b>	5%
	Submitted works	
2	<b>nith on 2022-06-08</b>	1%
	Submitted works	
3	<b>nith on 2022-07-04</b>	<1%
	Submitted works	
4	<b>nith on 2021-05-04</b>	<1%
	Submitted works	
5	<b>National Institute of Technology, Hamirpur on 2018-05-18</b>	<1%
	Submitted works	
6	<b>DevDatt Pathak, Subrata Kushari, SaikatRanjan Maity, Lokeswar Patnai...</b>	<1%
	Crossref	
7	<b>University of Hertfordshire on 2022-08-22</b>	<1%
	Submitted works	
8	<b>University of Bolton on 2022-01-12</b>	<1%
	Submitted works	



9	sageuniversity.in	Internet	<1%
10	"Recent Advances in Materials and Modern Manufacturing", Springer S...	Crossref	<1%
11	University of Hertfordshire on 2022-01-02	Submitted works	<1%
12	ijisrt.com	Internet	<1%
13	University of Western Sydney on 2020-10-29	Submitted works	<1%
14	"Advances in Lightweight Materials and Structures", Springer Science a...	Crossref	<1%
15	National Institute of Technology, Hamirpur on 2017-07-17	Submitted works	<1%
16	Abhishek Agarwal, Linda Mthembu. "Modelling and FE Simulation of H...	Crossref	<1%
17	uokerbala.edu.iq	Internet	<1%
18	nith on 2023-05-16	Submitted works	<1%
19	nith on 2022-06-03	Submitted works	<1%
20	maleliit.ee	Internet	<1%

21	Institute of Graduate Studies, UiTM on 2013-01-27	<1%
	Submitted works	
22	Jawaharlal Nehru Technological University on 2013-08-14	<1%
	Submitted works	
23	The University of the West of Scotland on 2023-03-31	<1%
	Submitted works	
24	University of Huddersfield on 2018-04-27	<1%
	Submitted works	
25	nith on 2022-06-03	<1%
	Submitted works	
26	nith on 2022-06-06	<1%
	Submitted works	
27	uir.unisa.ac.za	<1%
	Internet	
28	Central Queensland University on 2015-11-10	<1%
	Submitted works	
29	La Trobe University on 2020-10-03	<1%
	Submitted works	
30	University of Nottingham on 2012-08-31	<1%
	Submitted works	
31	eprints.usq.edu.au	<1%
	Internet	
32	gcris.iyte.edu.tr	<1%
	Internet	

33	link.umsl.edu	Internet	<1%
34	nith on 2021-05-04	Submitted works	<1%
35	nith on 2023-05-16	Submitted works	<1%
36	researchgate.net	Internet	<1%
37	Curtin University of Technology on 2017-10-01	Submitted works	<1%
38	Dr. B R Ambedkar National Institute of Technology, Jalandhar on 2020-...	Submitted works	<1%
39	Gyeongsang National University on 2020-07-30	Submitted works	<1%
40	Institute of Graduate Studies, UiTM on 2013-12-04	Submitted works	<1%
41	National Institute of Technology, Hamirpur on 2020-06-09	Submitted works	<1%
42	Siddaganga Institute of Technology on 2016-08-08	Submitted works	<1%
43	University of Hertfordshire on 2022-09-05	Submitted works	<1%
44	xajzkjdx.cn	Internet	<1%